REPUBLIC OF TURKEY
FIRAT UNIVERSITY
THE INSTITUTE OF NATURAL AND APPLIED SCIENCES
FACULTY OF SCIENCE

EXPERIMENTAL AND NUMERICAL ANALYSIS OF DEEP EXCAVATIONS

Bedar Rasul MAHMOOD
Master's Thesis
Department of Civil Engineering

JANUARY 2020

REPUBLIC OF TURKEY
FIRAT UNIVERSITY
THE INSTITUTE OF NATURAL AND APPLIED SCIENCES
FACULTY OF SCIENCE

Department of Civil Engineering

Master's Thesis

EXPERIMENTAL AND NUMERICAL ANALYSIS OF DEEP EXCAVATIONS

Thesis Author
Bedar Rasul MAHMOOD

Supervisor
Assoc Prof. Dr. H. Suha AKSOY

JANUARY 2020
ELAZIĞ

REPUBLIC OF TURKEY
FIRAT UNIVERSITY
GRADUATE SCHOOL OF NATURAL AND APPLIED SCIENCES

Civil Engineering Department
Geotechnical

Master Thesis

Title: Experimental and Numerical Analysis of Deep Excavations

Author: Bedar Rasul MAHMOOD

First Delivery: 04.12.2019

Date of Defense: 10.01.2020

THESIS APPROVAL

This thesis was prepared according to the rules of Firat University, Graduate School of Natural and Applied Sciences. It was evaluated by the jury members who have signed the following signatures and accepted unanimously because of the defense made available to the academic audiences.

		Signature
Advisor:	Assoc. Dr. H. Suha AKSOY Firat University, Faculty of Engineering	I Approved
Chairman:	Assoc. Dr.M.Salih KESKİN Dicle University, Faculty of Engineering	I Approved
Member:	Assoc. Dr.Muhammet KARATON Firat University, Faculty of Engineering	I Approved

This thesis was registered at the meeting of the board of directors of the institute on

/ / 20

Signature

Prof. Dr. Soner ÖZGEN

Director of the Institute

DECLARATION

This thesis “Experimental and numerical analysis of deep excavation” was writing according to the thesis writing rules of the Firat University, Graduate School of Natural and applied Sciences. All the information in my thesis is correct, scient eths in producing and presenting information that I have written in accordance with the rules, I have cited all the sources to receive the title of the data and the information that I have provided here. I have never used the data and information that provided here in order to get a degree in anywhere.

Bedar Rasul MAHMOOD

ELAZIĞ, 2020

PREFACE

The goal of this study is to investigate how the distance between foundation and sheet pile (L) and excavation depth (H_e) will affect deflection of the sheet pile and ultimate bearing capacity of the foundation model under axial loading for the same materials using relative density 10% only. All praises and thanks are to Allah, we seek His help and mercy, the Almighty, who has created the heavens and the earth, and brought into being deep darkness as well as light. On whom we definitely depend for sustenance, guidance and help.

I would like to thank my thesis advisor, in Civil Engineering Department Assoc. Prof. Dr. H. Suha Aksoy for his support, patience, motivation, all along my research. Who has always helped me and his door was always open, and was ready to help anytime when I got a problem about my research and wish him long life with gladness. I also want to thank Dr. Mesut GÖR and Res. Assist. Aykut ÖZPOLAT for their continuous help and support.This thesis was financially supported by BAP of Firat University.

At the end I have to express my deepest gratitude to my dear parents and my whole family for their continuous support, motivation and encouragement throughout my years of study, and they had a great role and always supported me to continue my studying

Bedar Rasul MAHMOOD
ELAZIĞ, 2020

TABLE OF CONTENTS

ABSTRACT

Experimental and Numerical Analysis of Deep Excavations

Bedar Rasul MAHMOOD

Master's Thesis

FIRAT UNIVERSITY
Graduate School of Natural and Applied Sciences

Department of Civil Engineering
January 2020, Pages: xv +77

The goal of this study is to investigate how the distance between foundation and sheet pile (L) and excavation depth (H_e) will affect deflection of the sheet pile and ultimate bearing capacity of the foundation model under axial loading for the same materials using relative density 10% only. Finite element method and statistical method was also used in this research to study the behaviour of the sheet pile, foundation model and lateral pressure under axial loading.

A sandbox which dimensions are 0.75x0.75x1m is filled with Dr=10% dry sand. A steel plate (12x12cm) is used as foundation model; steel sheet pile model with dimensions of 75x40x0.3 cm is used.

For this purpose 10 tests were performed to study the deflection of the sheet pile, bearing capacity of the soil and lateral pressure of the soil on the sheet pile, one of the test was performed without the sheet pile and other nine tests were performed with three different (L) and three different (H_e).

From the experimental results, time-deflection and load-deflection behavior of sheet pile and time-settlement and load-settlement behavior of the foundation are obtained. In order to determine the effects of L and H_e, these results are compared. It is observed that, when the distance between foundation and sheet pile (L) was increased the deflection of the sheet pile decreased and load capacity on the foundation is increased for the same excavation depth. It is also seen that when the excavation depth (H_e) was increased the deflection of the sheet pile increased and load capacity decreased for the same distance between foundation and sheet pile.

Also the results from Plaxis 3D finite element programs indicated that the deflection of the sheet pile model increases with increasing (H_e) and decreasing (L), and there is a good agreement between experimental results with finite element programs results.

Lateral pressures measured by using pressure transducers. These pressures analyzed statistically to derive a relation between test systems geometrical conditions and measured lateral pressures. An appropriate correlation (R^2=0.95) has been determined.

Key words: sheet pile model, foundation model, deflection of sheet pile, bearing capacity, finite elemente method.

ÖZET

Derin Kazıların Deneysel ve Nümerik Analizi

Bedar Rasul MAHMOOD

Yüksek Lisans Tezi

FIRAT ÜNİVERSİTESİ
Fen Bilimleri Enstitüsü

Inşaat Mühendisliği Anabilim Dalı
Ocak 2020, Sayfa: xv +77

Bu çalışmanın amacı, rölatif sıkılığı %10 olan bir zeminde, temel ile palplanş perde arasındaki mesafenin (L) ve kazı derinliğinin (H_e), palplanş perdenin deformasyonlarını ve model temelin taşıma kapasitesini nasıl etkileyeceğini araştırmaktır. Bu araştırmada palplanş perde davranışı, model temel davranışı ve eksenel yükleme neticesinde zemin kütlesinde oluşan yanal basınçları incelemek için model deneyleri yapılmış ve elde edilen sonuçlar sonlu elemanlar ve istatistiksel yöntemlerle analiz edilmiştir.

Boyutları 0.75x0.75x1m olan bir kum tankı, Dr =% 10 kuru kum ile doldurulmuştur. Temel modeli olarak bir çelik levha (12x12x2.5cm) kullanılmıştır. Palplanş perde ise 75x40x0.3 cm boyutlarında çelik saç ile modellenmiştir.

Bu amaçla, palplanş perde deformasyonlarını zeminin taşıma gücünü ve zeminin palplanş perdeye uyguladığı yanal basıncı incelemek için 10 deney yapılmıştır. Bir deney palplanş perde olmadan yapılmıştır ve diğer dokuz deney ise üç farklı farklı (L) ve üç farklı (H_e) değerleri kullanılarak yapılmıştır.

Deneysel sonuçlardan palplanş perdenin zaman-deformasyon ve yük-deformasyon davranışı ve model temelin zaman-oturma ve yük-oturma davranışları elde edilmiştir. L ve H_e'nin etkilerini belirlemek için bu sonuçlar karşılaştırılmıştır. Temel ile palplanş perde arasındaki mesafenin (L) arttırılması durumunda, aynı kazı derinliği için palplanş perde deformasyonlarının azaldığı ve temelin taşıma gücünün arttığı gözlenmiştir. Ayrıca, kazı derinliği (H_e) arttıkça, palplanş perde deformasyonlarının arttığı ve temel ile palplanş perde arasındaki aynı mesafe için taşıma gücünün azaldığı belirlenmiştir.

Ayrıca Plaxis 3D sonlu elemanlar programlarından elde edilen sonuçlar, model palplanş perde deformasyonunun, artan (H_e) ile ve azalan (L) ile arttığını göstermiştir. Sonlu elemanlar analizi sonuçları ile deneysel sonuçlar arasında iyi bir uyum olduğunu görülmüştür.

Yanal zemin basınçları basınç transdüserleri kullanılarak ölçülmüştür. Bu basınçlar ile test sisteminin geometrik koşulları arasında bir ilişki kurmak için istatistiksel analiz yapılmıştır. Yapılan çoklu regresyon analizi neticesinde determinasyon katsayısı (R^2 = 0.95) olan bir bağıntı elde edilmiştir.

Anahtar kelimeler: palplanş perde modeli, temel modeli, palplanş perde deformasyonları, taşıma gücü, sonlu elemanlar yöntemi.

LIST OF FIGURES

LIST OF TABLES

Page No

LIST OF APPENDIX

Page No.

LIST OF ABBREVIATIONS

Symbols

B	: Length of foundation model
H_e	: Excavation depth
D	: Grain size
Dr	: Relative Density (%)
M	: Bending moment or force couple
P	: Single load value
p	: Uniform stress
σ_V	: Vertical stress
σh	: Horizontal stress
ϕ	: Internal Friction Angle of the Sand
δ	: Angle of friction between wall and earth
K	: Coefficient of Lateral Earth Pressure
K_p	: Rankine's Passive Earth Pressure Coefficient
K_a	: Rankine's Active Earth Pressure Coefficient
K_o	: Coefficient of Earth Pressure at Rest
ASTM	: American Society for Testing and Materials
C_c	: Coefficient of Curvature
C_u	: Coefficient of Uniformity
D_{10}	: Effective Grain Size
D_{30}	: Particle size at 30 % finer
D_{50}	: Median Grain Size
D_{60}	: Particle size at 60% finer
e	: Void Ratio
e_{max}	: Maximum Void Ratio
e_{min}	: Minimum Void Ratio
Gs	: Specific Gravity
SP	: Poorly Graded Sand
USCS	: Unified Soil Classification System
γ_d	: Dry density

γ	: Soil Unit Weight
Es	: Modulus of Elasticity of Soil
μ	: Poisson’s Ratio of Soil
D_{tank}	: Diameter or Short Dimension of Model Tank
LVDT	: Linear Variable Displacement Transducer
γ_d	: Dry Unit Weight
G_s	: Specific Gravity
$\gamma_{d\ min}$	: Minimum Dry Unit Weight
$\gamma_{d\ max}$	: Maximum Dry Unit Weight
D_{max}	: Maximum Grain Size
D_{min}	: Minimum Grain Size
F	: Anchorage force

1. INTRODUCTION

The need for urban construction involving deep excavations to build foundations and underground infrastructure such as rapid mass transit and tunnels for cutting and recovery continues to increase as a result of rapid urbanization. Relaxing the stress caused by these deep excavations can lead to excessive movement of the lateral surface. The interaction between these lateral ground motions and the current surrounding pile bases creates an additional load. Such new loads will cause further bending moments and lateral deflections on existing foundations near piles. They must be taken into account in order to ensure the credibility of the piles as well as the institutions we support [1]. Determining the stress / deflection characteristics that may occur in the ground mass under the applied loads in the solution of many engineering problems is necessary. Stress and displacement are directly related to the stress / deflection properties of the earth. Since the earth does not show a linear change, it is difficult to reach a realistic solution. It is considered as homogeneous and isotropic by using elasticity theory in application because of this feature of the soil. At the moment of stress values lower than the collapse of the ground; the ground shows linear behavior. To investigate its nonlinear behavior, it is essential to analyze the finite element method by considering the heterogeneous and anisotropic features of the soil. [2].The effects of sheet-pile walls on water insulation to be investigated experimentally is necessary in the literature researches. It has been realized that the transportation of the earth weight of the sheet-pile walls are not experimentally investigated. The behavior of the sheet-pile walls on the cohesionless ground under the earth and foundation load was investigated experimentally [3].

2. SHEET-PILE WALLS

Sheet-pile walls are materials used in order to hold an earth weight, water-impermeable vertical continuous walls, which are formed by wood, reinforced concrete, steel and vinyl in a series of elements that are inserted into the earth. Sheet-pile walls can be taken into account as a beam which is located in the vertical direction as a static method because they can hold some of the horizontal loads coming from the earth and very little of the vertical loads. As a cross section, sheet-piles' width is very high compared to their length, they are structural elements. Sheet-pile walls are used in the construction of quay walls, wave breakers, retaining structures and similar structures, as well as to keep the rain and groundwater away from the foundation pit during construction, to prevent the seepage of the groundwater in the water relief structures, to increase the stability of the structures. They are used especially in coastal structures and foundation excavations. Special cross sections are steel, vinyl, wood or reinforced concrete elements. The lamp is tied to the floor in the form of a dowel and forms a continuous shear wall. The aim is to meet the ground and/or water loads. They generally constitute temporary resting structures and after the completion of the study they are used again [4].

For many purposes, they are widely used, such as:

- Huge buildings and sea side.
- Protection against erosion.
- Stabilize the soil's slopes.
- Retention of trenches walls and other excavations and cofferdams.

It is generally classified as anchored sheet piles or cantilevered sheet piles that are used for retaining walls. The sheet piles are made of different material forms such as wooden sheet piles, vinyl sheet piles, concrete sheet piles, steel sheet piles and aluminum sheet piles. There are various uses for these different materials and Figure 2.1 show the use of sheet pile. [5].

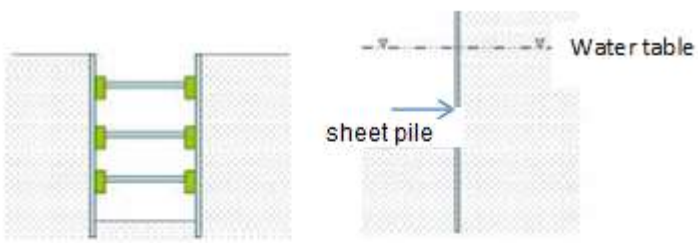

Figure 2.1. Schematic representation of sheet-pile[5]

The development, which provides an advantageous contribution to the sheet-pile industry, is the use of vinyl panels in 1989. Impervious plug-in vinyl panels have become an attractive technology for stopping or maintaining contaminated groundwater in the environmental industry. Sheet-piles are used as; coffer-dam, retaining walls, wave breakers, water sediments for many years [4].

The advantages of sheet-pile walls are:

• Excavation transport; without excavation is required and eliminates the problem of finding a dump.

• If necessary, or if desired, the sheet-piles can be removed later.

• They are fast, economical and safe.

• Topography and groundwater depth are little effective [6].

Sheet pile walls are constructed by:

1. Set up a series of sheet piles and ensure that the sheet piles fit into each other.
2. Drive the sheet to the desired depth (or vibrate).
3. Running the second sheet pile with the locks between the first sheet pile and the second "locked".
4. Repeat steps 2 and 3 until the wall perimeter is done.
5. When using more complex shapes, use connector components**.** [7].

2.1. Theories of Rankine (1857) and Coulomb (1776)

While Rankine Theory (RT) accepts the friction angle between the back of the structure and the earth as 0 RT; The Coulomb Theory (CT) takes into account the friction. RT, provide easier application since it takes into account stratified earth, cohesive floor, underground water conditions. While RT is giving lateral earth pressure distribution; CT yields the resultant force and Figure 2.2 show the stress of the earth.

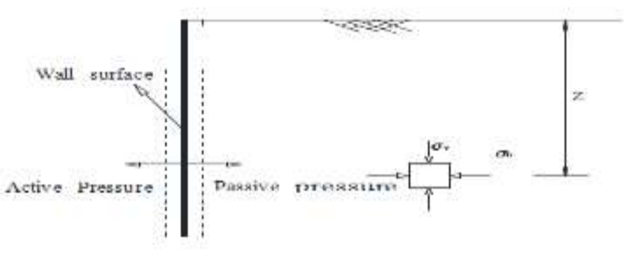

Figure 2.2. Internal stresses on earth [7]

Earth mass is accepted as homogeneous and isotropic. Considered depth of z; σ_v refers to vertical tension, σ_h horizontal stress. The ratio of vertical stress to horizontal stress gives K_0 the earth pressure coefficient in resting. It was accepted that there was no deflection in the horizontal direction.

$$\sigma_h \rightarrow \sigma_3$$

$$\sigma_v \rightarrow \sigma_1$$

Stresses on the earth that we call A and B during the wall movement, the active, passive earth pressures in cohesionless earth, according to the Rankine theory, can be seen as in Figure 2.3;

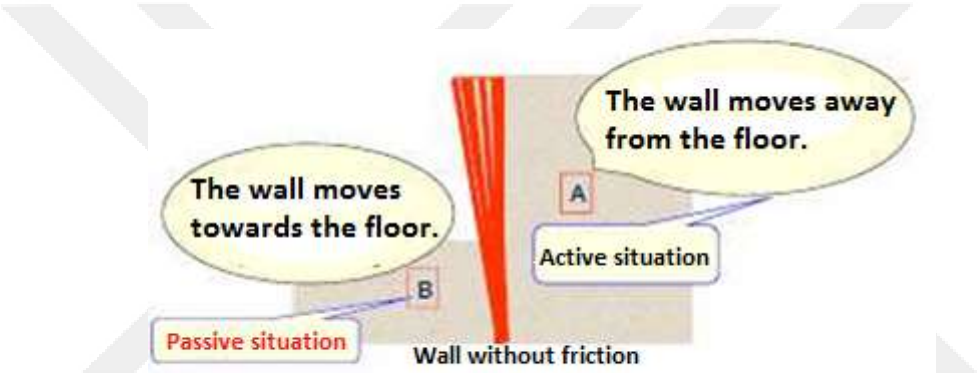

Figure 2.3. Formation of active and passive pressure on ground [8]

$\sigma v' = \sigma z$, $\sigma h' = K_0$, $\sigma v' = K_0\ \sigma z$, $\sigma v'$ values stay equal and $\sigma h'$ value will decrease until yield occurs. Because the wall moves in a direction away from the ground that shown in Figure 2.4 and Figure 2.5.

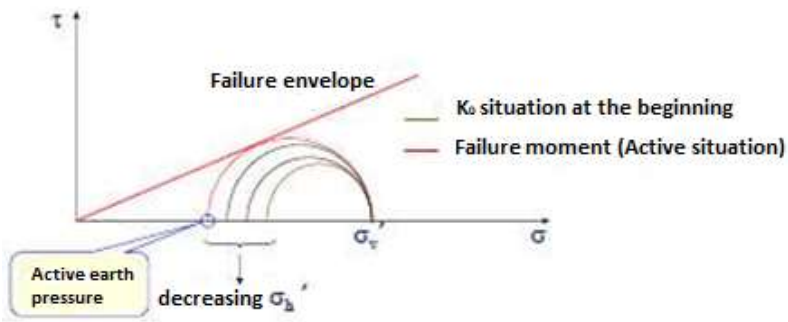

Figure 2.4. Active pressure graph [8]

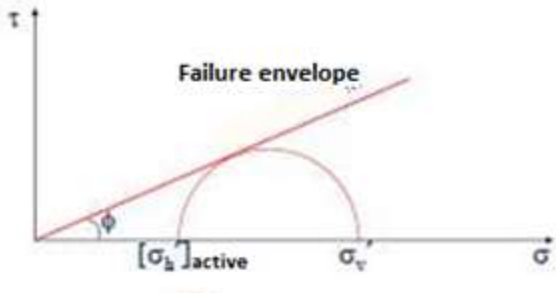

Figure 2.5. Rankine active earth pressure coefficient chart [8]

$$[\sigma_h^{'}]active = K_A \sigma_v^{'}$$

$$K_A = \frac{1+sin\varphi}{1-sin\varphi} = tan^2(45-\phi/2)$$

On the cohesive soils, the active earth pressure is the same as the one in non-cohesive soils. The only difference between the two is that the C coefficient is greater than zero in cohesive soils as shown in Figure 2.6, Figure 2.7 and 2.8.

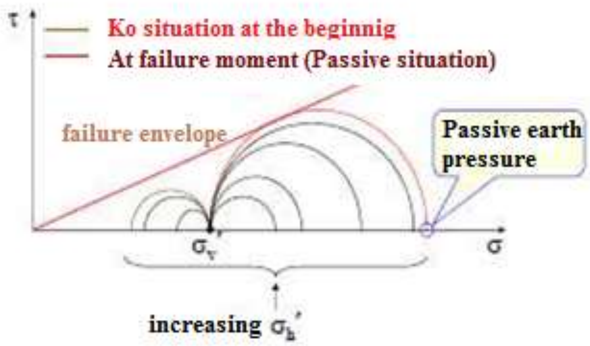

Figure 2.6. Passive earth pressure [8]

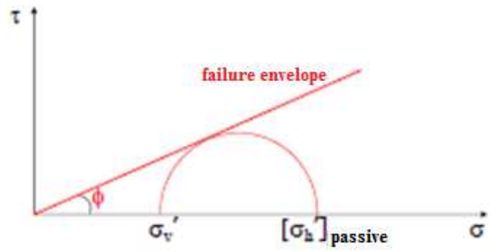

Figure 2.7 Rankine. passive earth pressure coefficient chart [8]

$[\sigma_h{}'] passive = K_P \sigma_v{}'$

$$K_p = \frac{1+sin\varphi}{1-sin\varphi} = \tan^2(45+\phi/2)$$

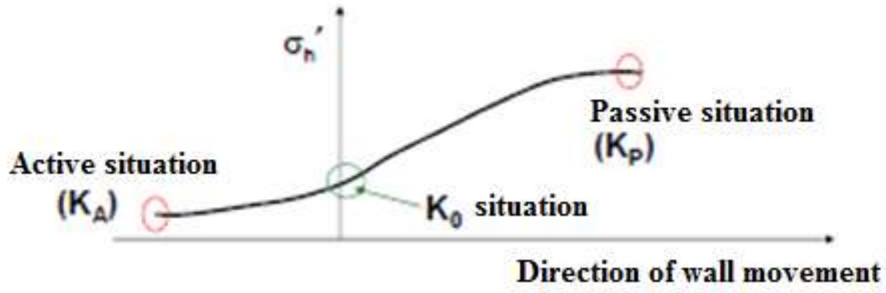

Figure 2.8. Distribution of earth pressures in non-cohesive soil [8]

The active and passive earth pressure according to the Rankine theory is calculated by following equation

$$[\sigma_h{}'] active = K_A \sigma_v{}' - 2c\sqrt{K_A}$$
$$[\sigma_h{}'] passive = K_p \sigma_v{}' + 2c\sqrt{K_p}$$

On the other hand, in the Coulomb theory, the wall considered the balance of the floating earth mass formed behind the wall while moving forward or backward. On the non-cohesive soils, it is assumed that the mass sliding from behind the wall is triangular (wedge). The earth is accepted to be homogeneous and isotropic, and the sliding surface is considered to be planar. Between the wall and the earth, the friction force is taken into consideration. And these friction forces are taken into consideration to be uniformly distributed along the sliding surface. The roughness of the back of the wall is the most important specification of the Coulomb theory. For the active situation (when the wall was moving forward) on cohesionless floors, downward movement (slipping) of the triangular wedge formed at the rear was taken into consideration in the Coulomb theory that shown in the Figure 2.9.

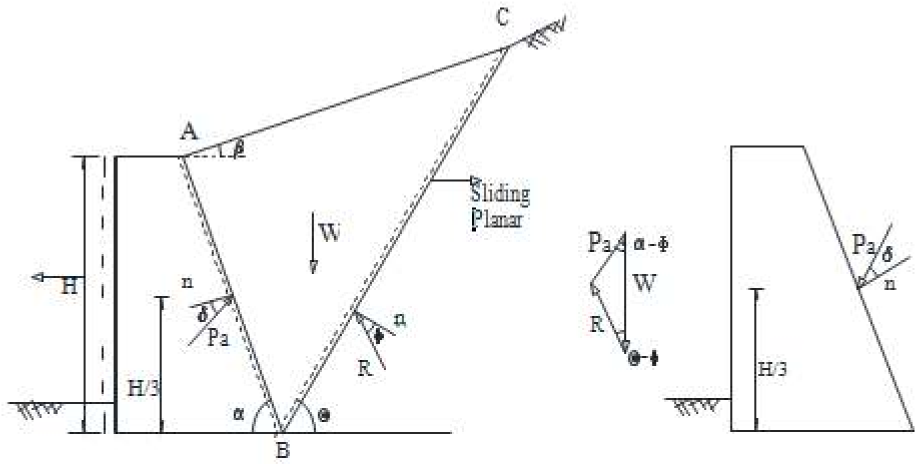

Figure 2.9. The mass movement on the floor according to coulomb theory [8]

The triangular wedge moves upward when the wall moves backwards in the passive state for non-cohesive floors and can be seen in Figure 2.10. [8]

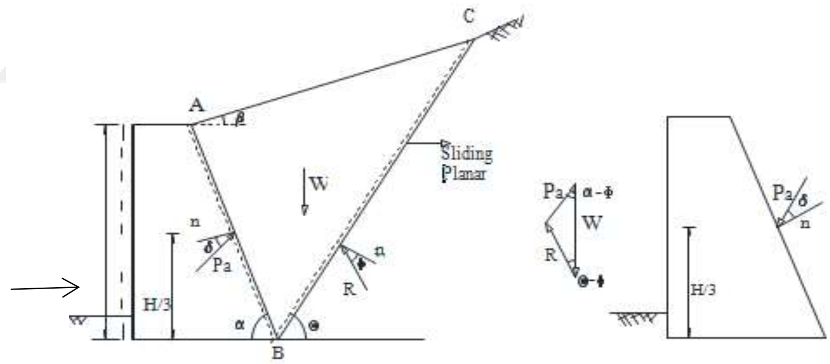

Figure 2.10. Calculation by coulomb theory [8]

$$P_P = \frac{1}{2}\gamma.H^2.K_P$$

$$K_p = \frac{sin^2(\alpha - \phi))}{sin^2\alpha.sin(\alpha - \delta)\left[1 - \sqrt{\frac{sin(\phi + \delta)sin(\phi - \beta)}{sin(\alpha - \delta)sin(\alpha + \beta)}}\right]^2}$$

2.2. Types of Sheet-Pile Walls

Sheet-pile walls are divided into 5 groups: wood, concrete, steel, vinyl and Aluminum.

2.2.1. Wooden Sheet-pile

During the construction of the foundations of the building as well as elements of the buildings on the earth, wooden sheet-pile walls are used as auxiliary structures. Nevertheless, their usage types are limited, provided that they are permanently below the deepest water or groundwater that may occur. They cannot be used on earth which contains structure residues. The plates are processed in a variety of ways, depending on the driving depth, the structure of the floor and what the sheet-pile walls will serve. As the wooden sheet-pile may be damaged, it cannot be used on the rock earth and on the earth which is full of building debris, Figure 2.11 and 2.12 shows the sample of wooden sheet pile. [9]

Figure 2.11. Wooden sheet-pile wall [9]

Figure 2.12. Wooden sheet-pile wall [9]

2.2.2. Concrete Sheet-pile

Concrete sheet-piles can be manufactured to the desired cross-section and size so that they can withstand the service loads and the loads that will affect during the construction period. These kinds of sheet-piles are heavy and their volumes are large. For that matter, during their transport and crashing, sheet-piles can cause problems. At a distance of one third, the short concrete sheet-piles can be transported from the top of the sheet-pile. In order to carry long sheet-piles, two or more transport points must be fastened. According to their intended use, they can be constructed to carry bending stresses. Moreover, in order to prevent additional loading during transport and driving reinforcements must be installed, Figure 2.13 show the sample of concrete sheet pile. [9]

Figure 2.13. Concrete sheet-pile wall [9]

2.2.3. Steel Sheet-pile

Because of the fact that wood and reinforced concrete sheet-piles in the rough stone earth and the wooden sheet-piles used to keep them away from the foundation pit cannot be reused, it has been found more suitable using steel sheet-piles. Steel sheet-piles are manufactured of cast iron which is interlocking. In this way, sheet-piles are avoided from being in the wrong signpost by the neighboring sheet-pile which has been punched and the sheet-piles are held by the ones next to them. The lock of this steel sheet should be at upmost tightness but movable. The ability of sheet-piles to move allows them to be pinned to a curve. The cross-sectional shapes of steel sheet-piles have very different types, Figure 2.14 show the sample of steel sheet pile. [9].

Figure 2.14. Steel sheet-pile wall [9]

2.2.4. Vinyl Sheet-pile

Vinyl panels started to be used in this area. Due to its easy to carry and practical application, its light weight is more advantageous than other materials, by way of lock connections, sealing is very high, because of its material specifications, in order to protect natural shore lines, it can be easily shaped and used in a practical way. Protection does not need maintenance for this reason, it is quite resistant to chemicals, sea water etc. It can perform its duties in the field without requiring maintenance for up to 50 years, Figure 2.15 and Figure 2.16 shows the saple of vinyl sheet pile. [9].

Figure 2.15. Vinyl sheet-pile wall [9]

Figure 2.16. Vinyl sheet-pile wall [9]

2.2.5. Aluminum sheet pile

Aluminum sheet piles have steel-like sections. It is made of alloy 6061 and is frequently used anodized, painted or visible. Aluminum is 100% recyclable, durable, and air, water, extreme temperatures, and chemicals resistant to corrosion, but more expensive than other typesFigure 2.17 and Figure 2.18 shows the sample of aluminum sheet pile. [9].

Figure 2.17. Aluminum sheet-pile wall

Figure 2.18. Aluminum sheet-pile wall

2.3. Sheet-pile Construction Methods

In earth retention works, sheet-pile walls are widely used. This may be a temporary or permanent work. More than half of the wall is embedded under the excavation height. This level creates horizontal stresses on the ground held by the wall and these stresses are met on the side of the embedded part. There are stresses on both sides of the embedded section due to earth impulse. In the case of very large excavations, near the top of the wall, more anchoring is used. Cantilever sheet-piles are usually used in temporary works, while anchored walls are used in permanent works. It is also displayed these two types of sheet-pile wall form in Figure 2.19. Evidently, only on the side of the soil that is embedded, the stability of the cantilever sheet-pile wall is supplied. On the other hand, the stability of the anchored wall is provided both on the earth and on the anchor side.

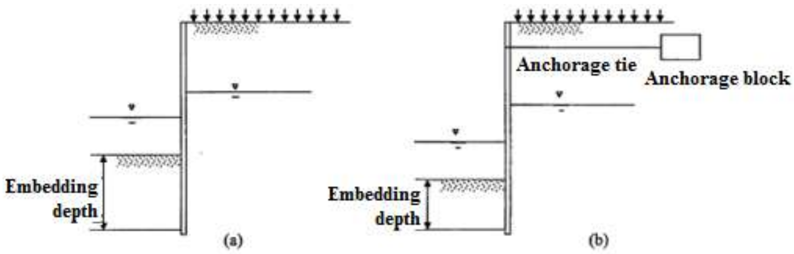

Figure 2.19. Sheet-pile wall: (a) cantilever (b) anchored [9]

Cantilever sheet-pile wall are used for lower heights and consist of heavier material than anchored wall. It should also be taken into account that there will be capillary tension changes during the service life of the wall on the cohesive earth. These changes can have harmful effects on the ground strength parameters. It is difficult to define the mixed relationship between the soil and the sheet-pile. In this case, various earth models are used to quantify net soil stress. In general, maximum bending moment and shear force values obtained from these methods are accepted. But these results cannot be used to predict ground movements.

In the numerical analysis of the sheet-pile wall, soil models can be applied considering the only part under the ground, such as the beam under the soil where the stress is zero.

According to the application form;

1. Cantilever
2. Anchored:

- Dead Anchored
- Pre-tensioning Anchored

Depending on the ground support:

Depending on the floor bearing:

- Buried Bearing
  - Cantilever
  - Anchored (Argillaceous soil)
- Free Bearing
  - Anchored (Sand)

2.3.1. Cantilever Sheet-piles

In cantilever sheet-piles, earth impulse which is in the back will be met in embedded depth by passive pressure which will occur in front of the pile and earth impulse in piles which are connected to back will be met both bond and passive pressure. Cantilever sheet-piles are structures which are enough to form a vertical cantilever by folding them to the earth sufficiently. The cantilever walls generally show large horizontal displacement and are rapidly but adversely affected by scour and erosion in front of the wall. Because the resistance to horizontal earth impulse is composed of passive stresses in the embedded depth, the penetration depths are large and therefore the bending and stresses reach large dimensions. Therefore, the cantilever wall heights are usually limited to 5 (m) and Figure 2.20 show the cantilever sheet pile.

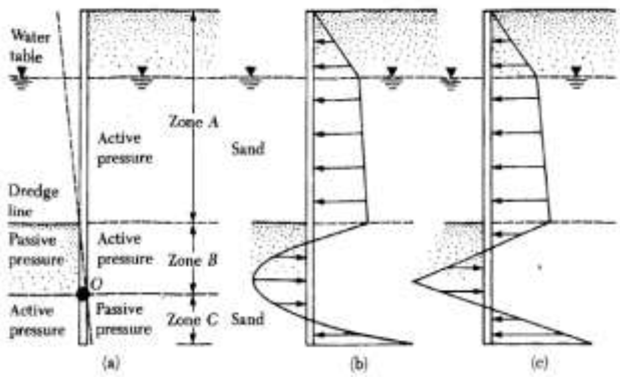

Figure 2.20. Cantilever sheet piles [8]

Sandy Earth Cantilever Sheet-piles

The active and passive pressures on both sides should be considered in order to find the net lateral pressure at the embedding depth on the pivot point of the sheet-pile that can be calculated by the equation below and Figure 2.21 show the example of sandy earth cantilever sheet pile.

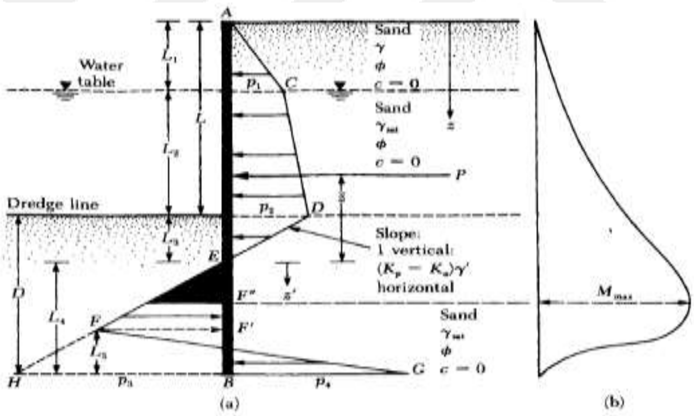

Figure 2.21. Cantilever sheet piles: (a) variation of net pressure diagram; (b) variation of moment [8]

$$p_a = \left[\gamma L_1 + \gamma' L_2 + \gamma'\left(z - L_1 - L_2\right)\right]K_a$$
$$p_a = \gamma'\left(z - L_1 - L_2\right)K_p$$

K_P = Rankine passive ground pressure coefficient = $\tan^2\left(45 + \phi/2\right)$

$$p = p_a - p_p = (\gamma L_1 + \gamma' L_2)K_a + \gamma'\left(z - L_1 - L_2\right)(K_p - K_a)$$
$$= p_2 - \gamma'(z - L)(K_p - K_a)$$
$$L = L_1 + L_2$$

Net pressure in L_3 depth p = 0;

$$p_2 - \gamma^{'}(z-L)(K_p - K_a) = 0$$

Or

$$(z-L) = L_3 = \frac{p_2}{\gamma^{'}(K_p - K_a)}$$

This equality shows incline of DEF.

Using the above equation, P_3 pressure can be written;

$$H\overline{B} = p_3 = L_4(K_p - K_a)\gamma^{'}$$

The passive pressure p_p at the base of the sheet-pile is from the right to the left.

This depth;

z = L + D so;

$$p_p = \left(\gamma L_1 + \gamma^{'} L_2 + \gamma^{'} D\right) K_p$$

In the same depth;

$$p_a = \gamma^{'} D K_a$$

Net horizontal pressure at the lower end of the sheet-pile;

$$p_p - p_a = p_4 = \left(\gamma L_1 + \gamma^{'} L_2\right) K_p + \gamma^{'} D(K_p - K_a)$$
$$= p_5 + \gamma^{'} L_4 (K_p - K_a)$$
$$p_5 = \left(\gamma L_1 + \gamma^{'} L_2\right) K_p + \gamma^{'} L_3 (K_p - K_a)$$
$$D = L_3 + L_4$$

Considering the static balance for the stability of the sheet-pile as shown in the Figure 2.22.

$$\sum FH = 0$$
$$\sum MB = 0$$

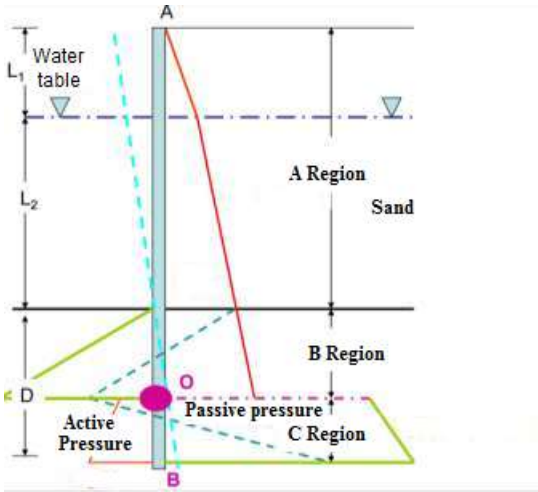

Figure 2.22. Sandy earth cantilever sheet-piles stability [8]

The sum of the fields of pressure diagrams;

$ACDE - EFHB + FHBG = 0$ Or:

$$p - \frac{1}{2} p_3 L_4 + \frac{1}{3} L_4 (p_3 + p_4) = 0$$

p = If the sum of the moments according to the B point of the ACDE field is written ;

$$p(L_4 + \bar{z}) - (\frac{1}{2} L_4 p_3)(\frac{L_4}{3}) + \frac{1}{2} L_5 (p_3 + p_4)(\frac{L_5}{3}) = 0$$

$$L_5 = \frac{p_3 L_4 - 2p}{p_3 + p_4}$$

If the values written instead of moment above;

$$L_4^4 + A_1 L_4^3 - A_2 L_4^2 - A_3 L_4 - A_4 = 0$$

$$A_1 = \frac{p_5}{\gamma^{'} (K_p - K_a)}$$

$$A_2 = \frac{8p}{\gamma^{'} (K_p - K_a)}$$

$$A_3 = \frac{6p[2\bar{z}\gamma^{'} (K_p - K_a) + p_5]}{\gamma^{'2} (K_p - K_a)^2}$$

$$A_4 = \frac{p[6\bar{z}p_5 + 4p]}{\gamma'^2 (K_p - K_a)^2}$$

Calculating Maximum Moment;

$$p = \frac{1}{2}(z')^2 (K_p - K_a)\gamma'$$

Or

$$z' = \sqrt{\frac{2p}{(K_p - K_a)\gamma'}}$$

$$M_{\max} = p(\bar{z} + z') - [\frac{1}{2}\gamma'(z')^2 (K_p - K_a)\frac{1}{3}z'$$

Cantilever Sheet-Piles on Clay Floors

In cantilever sheet-piles on clay floor, earth impulse which is in the back will be met in embedded depth by passive pressure which will occur in front of the pile and earth impulse in piles which are connected to back will be met both bond and passive pressure as shown in the Figure 2.23.[8]

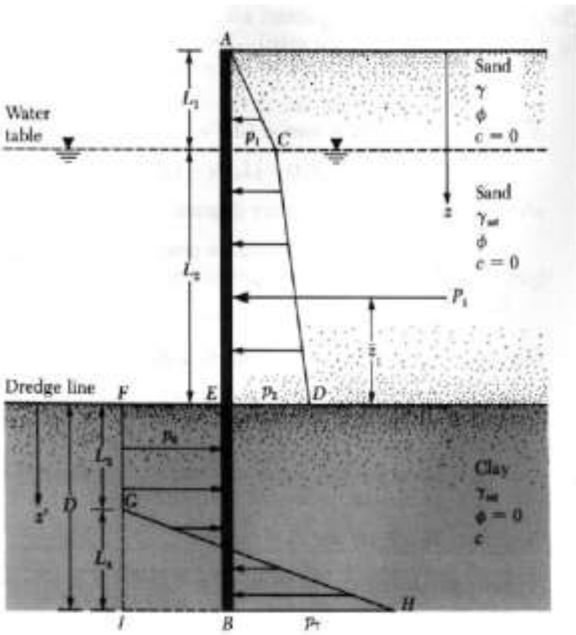

Figure 2.23. Cantilever sheet-piles on clay floors [8]

As ∑FH = 0; the area of the ACDE area - EFIB area + GIH from the pressure diagram areas = 0

$$p_1 - [4c - (\gamma L_1 + \gamma^{'} L_2)]D + \frac{1}{2} L_4 [4c - (\gamma L_1 + \gamma^{'} L_2) + 4c + (\gamma L_1 + \gamma^{'} L_2)] = 0$$

If the sum of moments according to point B is written;

$$p_1 (D + \bar{z}_1) - [4c - (\gamma L_1 + \gamma^{'} L_2)]\frac{D^2}{2} + \frac{1}{2} L_4 (8c)(\frac{L_4}{3}) = 0$$

$$L_4 = \frac{[4c - (\gamma L_1 + \gamma^{'} L_2)]D - P_1}{4c}$$

$\bar{z}_1$ = ABCD pressure diagram, the vertical distance of the center of gravity.

$$D^2 [4c - (\gamma L_1 + \gamma^{'} L_2)] - 2Dp_1 - \frac{p_1 (p_1 + 12c\bar{z}_1)}{(\gamma L_1 + \gamma^{'} L_2) + 2c} = 0$$

$$D_{actual} = 1.4 - 1.6(D_{theorical})$$

Calculating Maximum Moment;

To calculate the maximum torque, the point where the cutting force is zero is found:

$$p_1 - p_6 z^{'}$$

Or

$$z^{'} = \frac{p_1}{p_6}$$

$$M_{\max} = p(\bar{z} + z_1^{'}) - \frac{p_6 z^{'2}}{2}$$

2.3.2. Anchored Sheet-piles

On the state that the excavation depth is greater than 6 m, the cantilever sheet-piles are not economical and that’s why in such cases, the anchor sheet-piles are used. Anchored sheet-piles reduce the driving depth and wall deflections, as shown in the Figure 2.24 (a) and Figure 2.24 (b).

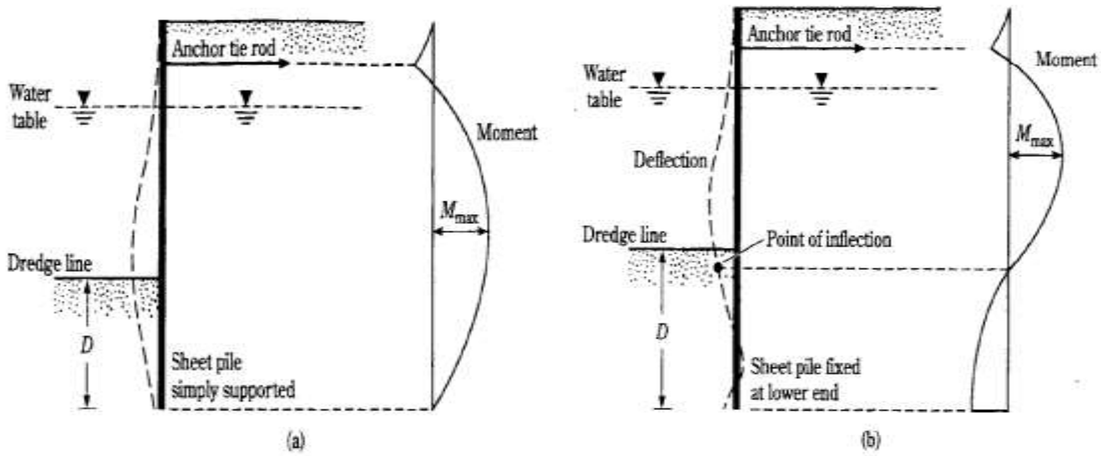

Figure 2.24. Anchored sheet-pile (a) with free bearing (b) with buried bearing

Anchored Sheet-pile with Free Bearing in Sand

The anchored sheet pile with free bearing in sand can be investigated with the equation below and Figure 2.25 show the example of the anchored with free bearing in sand.

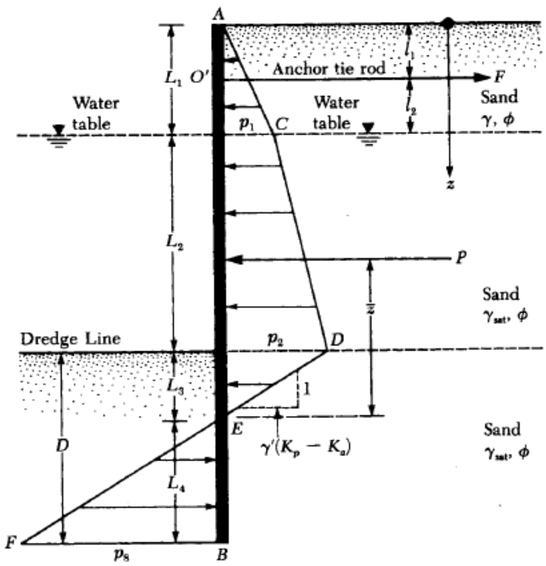

Figure 2.25. Anchored sheet-pile with free bearing in sand [8]

$z = L_1$ Depth $p_1 = \gamma L_1 K_a$

$z = L_1 + L_2$,De $p_2 = (\gamma L_1 + \gamma' L_2) K_a$

$z = L_1 + L_2 + L_3$,Depth $p = 0$ (E point)

$$L_3 = \frac{p_2}{\gamma^{'}(K_p - K_a)}$$

$z = L_1 + L_2 + L_3 + L_4$, Depth

$$p_8 = \gamma^{'}(K_p - K_a)L_4$$

Slope of DEF; $1/\gamma^{'}(K_p - K_a)$

Considering the static balance for the stability of the sheet-pile;

∑FH=0 ∑MB=0

Sum of pressure diagrams for horizontal balance;

ACDE – EBF - F = 0

F = Tension in Anchor / unit length

$$p - \frac{1}{2}p_8 L_4 - F = 0$$

Or;

$$F = p - \frac{1}{2}[\gamma^{'}(K_p - K_a)L_4^2$$

p =Area of ACDE pressure diagram
If the moment according to O' point is taken

$$\sum MO' = 0$$

$$-p[(L_1 + L_2 + L_3) - (\bar{z} + l_1)] + \frac{1}{2}[\gamma^{'}(K_p - K_a)L_4{}^2(l_2 + L_2 + L_3 + \frac{2}{3}L_4) = 0$$

Or

$$L_4{}^3 + 1.5L_4{}^2(l_2 + L_2 + L_3) - \frac{3p[(L_1 + L_2 + L_3) - (\bar{z} + l_1)]}{\gamma^{'}(K_p - K_a)} = 0$$

The above equation can be solved by trial and error method. Hereunder, theoretical driving depth;

$D_{theoretical} = L_3 + L_4$

The theoretical driving depth is increased by 30% to 40% in practice;

$D_{actual} = 1.3 - 1.4 D_{theoretical}$

Some engineers prefer to divide the passive earth pressure into a safety number instead of the actual driving depth.

$$K_{p(design)} = K_p / G_s$$

Max. Theoretical moment is between $z = L_1$ and $z = L_1 + L_2$ depth. From cutting force = 0 value of "z depth" can be found and M_{max} can be calculated as well.

$$\frac{1}{2} p_1 L_1 - F + p_1 (z - L_1) K_a (z - L_1)^2 = 0$$

Anchored Sheet-pile with Free Bearing in Clay

The anchored sheet pile with free bearing in clay can be investigated with the equation below and Figure 2.26 show the example of the anchored with free bearing in clay.

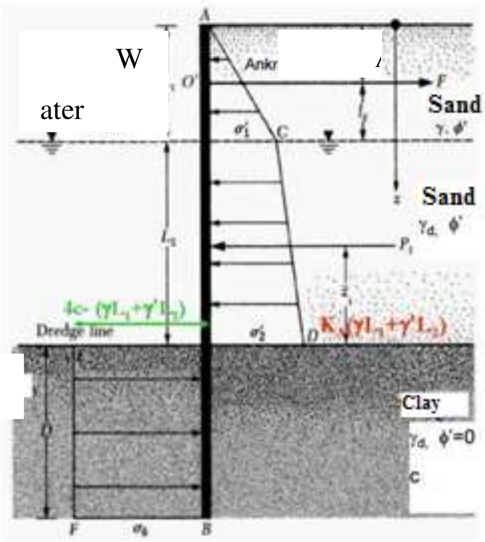

Figure 2.26. Anchored sheet-pile with free bearing in clay

From $z = L_1 + L_2$ depth

Until $z = L_1 + L_2 + D$

$$p_6 = 4c - (\gamma L_1 + \gamma' L_2)$$

From horizontal force

$$p_1 - p_6 = F$$

p_1 =ACD pressure diagram area

F=Anchored force (force/unit length)

If the moment according to O' point is taken;

$$\sum MO' = 0$$

$$p_1(L_1 + L_2 - l_1 - \bar{z}_1) - p_6 D(l_2 + L_2 + \frac{D}{2}) = 0$$

$$p_6 D^2 + 2p_6 D(L_1 + l_1) + 2p_1(L_1 + L_2 - l_1 - \bar{z}_1) = 0$$

In order to calculate the driving depth D, this equation is used.

Buried to Earth Anchored Sheet-pile

In the calculation of L3 and D for the solution of the anchored bearing with buried sheet-pile, the equivalent beam solution method is generally used that shown in Figure 2.27.

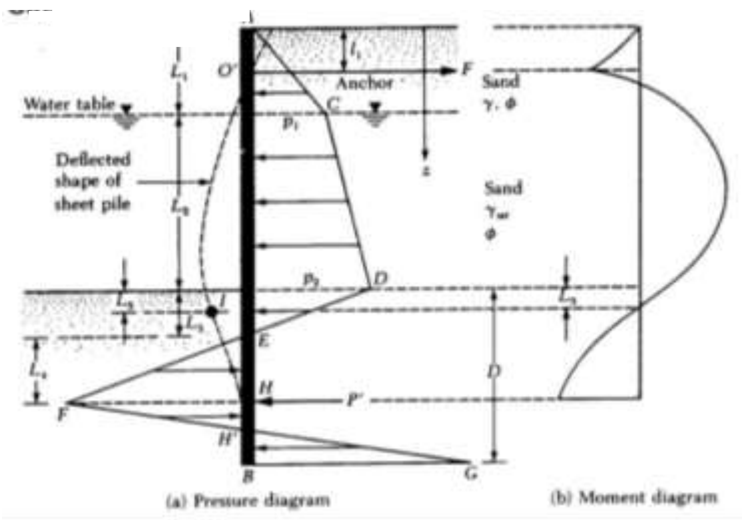

Figure 2.27. Pressure and moment diagram of anchored sheet-pile which is buried to earth [8]

The sheet-pile can be compared to a beam, as shown in Figure 2.28 below. In this beam, the T support is equivalent to the anchoring response (F) in the sheet-pile and the S point in the inflection point (I) is the equivalent of the Beam and Figure 2.28 show that..

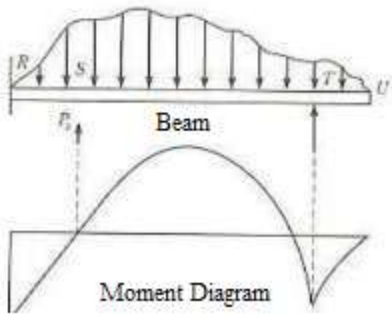

Figure 2.28. Method of equivalent beam [8]

In Design, the below path is followed:

1. L_5 is designated. From the table 2.1 below as a function of f, the L_5 angle of shearing resistance can be taken.
2. Table 2.1**.** Angles of shearing resistance

Table 2.1. Angles of shearing resistance

ϕ **(Angle)**	$\frac{L_5}{L_1 + L_2}$
30	0.08
35	0.03
40	0

3. $12 + L_2 + L_5 = L$ formula is the calculation of equivalent beam span.
4. In span, total load is measured with W. Span of the area between O' and I diagram.
5. $M_{max} = WL'^2 / 8$ is the calculation of maximum moment.
6. P is calculated by taking moment according to O'

$p' = \frac{1}{L'}$ (ACDJI moment area according to O')

7. D is calculated;

$$D = L_5 + 1.2\sqrt{\frac{6p'}{(K_p + K_a)\gamma'}}$$

8. F anchored force is calculated by taking moment according to I ,

$F = \frac{1}{L'}$ (ACDJI moment area according to I)

3. LITERATURE REVIEW

Liu, et al were studies on the use of sheet-pile walls to prevent settlements on the ground as a result of the earthquake. Experiments were performed on 50 cm thick soil. In order to cover the walls, the soil was fully enclosed. As a sheet-pile, a transparent vinyl sheet was used. As a result of the studies, it was found that the use of sheet-pile on non-liquefaction soils reduced seismic settlement [10].

For active sheet-piles events, because piles are directly affected by the presence of piles which exist and are related with earth movement, lateral forces which act on the sheet-piles are complex. For this reason, the solution for a single sheet-pile cannot be adapted for the solutions of the group sheet-piles. In a lot situation, single sheet-pile problems have been solved and in group effects, they can be solved by using some correction factors just like as single sheet-pile problems. Leung et al conducted centrifugation tests to analyze, respectively, the reaction of a single sheet pile between sand and clay excavations [11].

Ong et al found that the maximum induced bending moment and lateral deflection of the sheet-pile reduce exponentially with increasing distance from the excavation face and the provision of restraints at the pile head induce additional bending moments and shear forces[12].

O'Rouke found that due to the dissipation of excess interstitial pressure, the wall and the ground continued to move towards the excavation, even after the work was completed. As a result, even after the completion of the excavation, the bending moment and the lateral deflection of the pile increase with time. They defined a significant area of soil deflection, delineated by the wall and a line from the bottom of the clay layer to the surface of the soil, inclined 45˚ times to the wall [13].

Guo et al performed experiments on reduced sand models to research the piles ' activity due to lateral soil movements incorporating piles-supported axial loads. They concluded that the axial load imposed on a pile head appears to decrease the moment of bending, the soil reaction and the pile's lateral deflection [14, 15].

Design graphs by Poulos and Chen based on the results of a two-step analysis process. First the study of finite elements with plane deflection was used to obtain soil deflections due to excavations. The measured lateral ground movements were then used to conduct a sheet pile analysis based on the boundary element model. They researched factors of impact such as depth of excavation, rigidity and spacing of the support system, soil properties, and sheet pile properties such as sheet pile size, sheet pile width, sheet pile thickness, and total lateral deflection of a sheet pile adjacent to an undrained clay excavation. They also believed that excavations were both unsupported and strengthened [16, 17].

Recently, Chen and Poulos have developed theoretical methods for assessing the behavior of sheet piles subject to excavation-induced soil movement. They noticed that there were very limited field data available to test these theoretical approaches, as it is virtually impossible to use real piles in the field. Centrifugal design testing is an interesting way to study the problem [18].

Stewart et al had carried out centrifuge experiments to research the actions of stacked bridge abutments due to backfill loading that are subject to soil movement [19].

Torrabadella said there are many methods from the first half of the twentieth century to build sheet pile walls. Those initial ideas are ongoing and can be revised at the moment [20].

Calculations are required regardless of the method adopted to determine the balance of forces and horizontal moments formed along the wall and to identify the break point along the sheet pile wall and the depth of anchorage below the dredging line for false or anchored door-to-door walls by means of a geotechnical model. The second method, the technique of finite elements, was first suggested by (Morgenstern and Eisentein 1970) [21].

Uses the technique of finite elements to solve equations of rigidity. A sufficient knowledge of the soil's stress-strain behavior and its parameters is important because it indicates the soil-structure system's behavior. The main advantage of the anchored sheet pile wall when considering sheet pile walls that are cantilevered or anchored is its ability to reduce the sheet pile's embedding depth, thus increasing the excavation depth, which has a profitable effect on the structure [22].

The upper part is secured using anchoring systems consisting of tie rods and anchors to strengthen the strength of the high walls. This type of sheet pile wall is called an anchored sheet pile wall. The use of grounded sheet pile walls has maintained high soil and/or water levels around the world that are practically unsupported by gravity walls [23].

Miao et al. Have researched behind steel sheet piles a group of four concrete piles. After a few loading and unloading cycles, test results showed that pore water pressure increased in saturated and relatively loose embankments, resulting in an active stress loss in the lateral dispersion of liquefied sand. The tendency towards minimal potential energy in the liquefied soil has led to deflection of the sheet pile, bending moments and lateral deflection of the piles [24].

Soil anchors are slowly mounted to hold sheet piles during excavation. And found that behind the sheet piles it built an "armed earth zone" to form a retaining wall system around the excavation. As a result, deep excavations in a wide range of field conditions can be assisted [25].

Due to the complexity of the environment around the pits and the limited construction space, most pits with irregular geometries have been commonly used in a variety of practical engineering applications in recent years. For different excavations, the IPS soil retention method was applied [26, 27].

Sagaseta et al used Sagaseta (1987)'s proposed source-sink imaging technique to measure free ground motions. These calculated free-field movements are applied to the ground adjacent to the pile, where a series of springs or p-y curves represent the soil-pile interaction. They found that as the workload on the pile increases, the compaction of the excavation-induced pile increases, but the workload applied has little impact on the lateral response of the pile [28, 29, and 30].

In order to simulate the loads applied by an existing building using the finite difference method, Park et al analyzed the effect of excavations for a new pile cap adjacent to an axially loaded pile with different pressure on the soil surface. When the surface pressure is high, it has been found that significantly greater lateral movements and bending moments are induced in the pile. He showed that bending moments and shear forces are significant compared to those caused by induced vertical deflections due to induced lateral deflections [31].

The definition of the plane strain ratio (PSR), first proposed by Ou et al, is the ratio of a wall section wall's maximum deflection to the section's maximum deflection in conditions of plane deflection. For standard excavation in clay soils in Taipei, Taiwan, PSR values are calculated and evaluated [32].

During wall excavations, wall displacement amplitude and form are also influenced by the distance between the segment being examined and the excavation corner. The effect on displacement of the segment position is referred to as a three-dimensional effect or wedge effect. Several studies have studied the behavior of walls impacted by deep excavations, including the Clough and O'Rourke walls [32], Ou et al. [33, 34].

Most of these studies focused on clay excavations and few documented Nikolinakou et al sand excavations. They used the MIT soil model S1 to analyze sand excavations in Berlin, Germany, to conduct a feedback analysis. Nikolinakou et al's restraint and bracing systems and soil properties vary from the excavation case presented in his analysis [35].

Based on 18 excavation cases chosen to test the excavation behavior characteristics, the wedge effect was found to occur and the total lateral motion of the retaining structure was influenced by the length of the pit, according to a numerical analysis [36].

The excavation sequence plays a key role in regulating the response to deflection from the foundation in addition to structural restriction factors such as support size, excavation geometry, wall stiffness and diameter ratio [37].

Only a limited number of studies have concentrated on key issues such as thickness and sequence during concrete layered and blocked excavation, layered and blocked excavation measures were taken, benefiting from the time-space effect theory, which control the deflection induced by soil resistance, so as to reduce the retaining wall deflection. Finally, controlling deflection of the foundation pit was achieved [38, 39].

In this study, by foundation loading with the help of the hydraulic system, the excavation depth of the soil behind the sheet-pile wall and the distance of the foundation from the sheet-pile wall are changed; the deflections of the foundation are measured. The deflection measurements were taken from the 2 ends of the foundation and from the middle of the sheet pile. 0.75x0.75x1 meter sized semi-infinite medium to model the reservoir was used in the study. The foundation model was used in the dimensions of 12x12 cm. Lvdt devices were used in the measurements. Pressure transducers were used to measure the pressure of soil on the sheet-pile wall. According to the data obtained from the experiments using different excavation depths of soil behind sheet-pile and foundation distances; the time-deflection graphs and deflection-force, force-time graphs of the ground were plotted. These graphs were compared with each other and the effects of different sheet-pile depths and foundation distances were investigated.

Different excavation depth behind sheet-pile and foundation distances; the time-deflection graphs of the sheet-pile and the deflection-force graphs of the earth were plotted. These graphs were compared with each other and the effects of different sheet-pile depths and foundation distances were investigated.

4. EXPERIMENTAL STUDY

This chapter will provide an explanation of all the properties of the materials and equipment used in this study. Moreover, it will also explain more details about all test procedures which have been done for this study, such as direct shear test for determination internal friction angle (ϕ) of sand and the behavior of the sheet-pile walls in sandy soil were investigated experimentally. By loading the foundation with the help of the hydraulic system, the depth of the soil behind the sheet-pile and the distance of the foundation to the sheet-pile are changed; the deflection measurements were taken from the two edges of the foundation and the center of the sheet-pile. By using data logger it obtained data from the experiments using different depths of the soil behind the sheet-pile and foundation distances.

4.1. Features of Test system

In the study 0.75x0.75x1 meter sized which can model the half space medium was used. The foundation model was used in the dimensions of 12x12 cm. Measurements were made using the necessary calibrations of lvdt devices in Figure 4.1. In the experiment set, sand tank can be seen in Figure 4.2 (a, b), above the tank so that the sand can be poured as standard and sand can be filled from the desired height to the reservoir with the help of pipe. The sand tank is filled with sand by a bucket elevator system as shown in Figure 4.3 (a, b). Bucket elevator system is preferred to keep the sand as standard and not break it. A hydraulic system as shown in Figure 4.4 was used to model the loads in the test tank.

Figure 4.1. Lvdt measurement device

(a)

(b)

Figure 4.2. (a) And (b) Sand tank and raining hose

(a)

(b)

Figure 4.3.(a) And (b) Bucket elevator system

Figure 4.4. Hydraulic load system and load cell

Figure 4.5 (a, b) and 4.6 shows the brand of the data logger, load cell and lvdt devices.

(a) (b)

Figure 4.5. (a) Data logger (b) S type load cell

Figure 4.6. Lvdt

The brand of the devices**:**

- Data logger (Test Box 1001)
- S Type Load cell (Keli Brand)
- Lvdt (Opkon Brand)

4.2. Material Properties of Sand and Sheet-pile Wall

4.2.1. Sand Properties

The sand used in the experiments of this study was river sand with uniform gradation brought from the Murat River in Elazığ at Turkey. The sand has been washed and oven dried and sieved by passing 1 mm opening sieve and retained on the sieve #200 (0.075 mm). The sieve analyses and specific gravity tests were performed according to standards (ASTM D422-63 and ASTM D854-14) [41, 42]. Relative density of the sand was determined according to (ASTM D4254-16) [43]. The sand is classified as poorly graded sand (SP) according (USCS) which is refer to Unified Soil Classification System according to ASTM D2487. Figure 4.7 illustrates the grain size distribution curve of the sand. Physical properties of the sand are summarized in the table 4.1.

Table 4.1. Physical properties of the sand used in the study

Property	**Value**
Effective size, D_{10}, D_{30},D_{50}, D_{60} (mm)	0.19, 0.325, 0.475, 0.55
Coefficient of uniformity, C_u	2.895
Coefficient of curvature, C_c	0.980
Classification (USCS)	SP
Specific gravity, G_s	2.77
Maximum dry unit weight, γ_d (max.) kN/m^3	17.66
Minimum dry unit weight, γd (min.) kN/m^3	14.32
Maximum void ratio, e_{max}	0.898
Minimum void ratio, e_{min}	0.539
Maximum – Minimum grain size, D_{max}-D_{min} (mm)	1 - 0.074

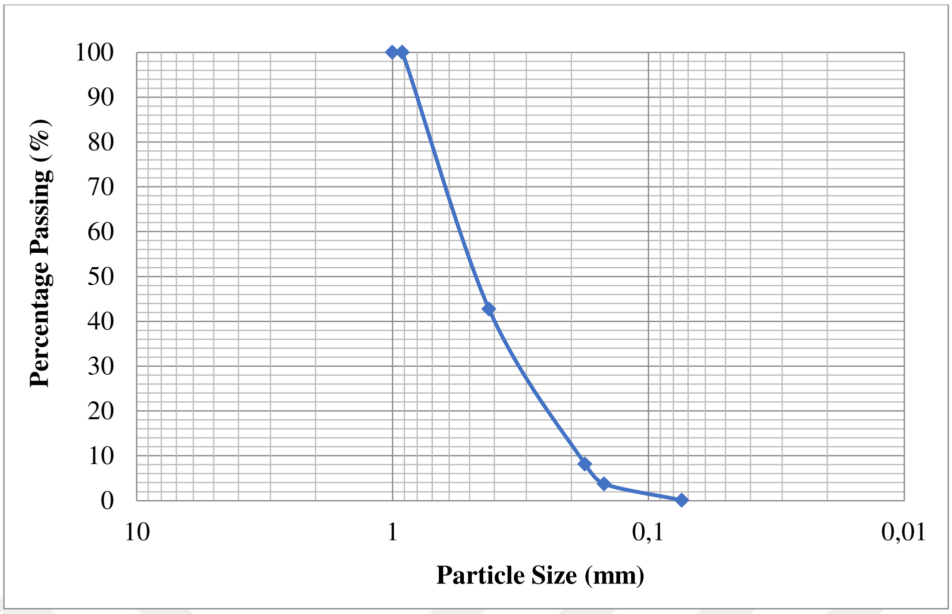

Figure 4.7. Grain size distribution of the sand

In Figure 4.8, a pre-made cup was used to determine the relative density, and a lot of experimentation tests were carried out. In Table 4.2, data which was obtained as a result of the tests is shown. In the test, 10% relative density was used.

Figure 4.8 Determination of relative density

Table 4.2. Dry unit weight and void ratio of the sand corresponding to relative density

Compaction Process	Average Dry Unit Weight(γ_d),(kN/m^3)	Void Ratio (e)	Relative Density (Dr,%)
The model sand usually pours from a height of 10 cm until the model tank is filled to a required depth.	14.6	0.86	10

Data which were obtained from experiments;

- For the loosest state; raining will be applied only from the height of 10cm. The hand compactor will not be used. Therefore, approximately Dr = 10% will be obtained.
- Only one relative density of the sand used in experiments for the internal friction angles is made as follows.

If $e_{min} = 0.539$, emax = 0.898, Dr = $\frac{0.898 - e}{0.898 - 0.539}$

$e_{10} = 0.86$

4.2.2. Direct Shear Test

In this study normal direct shear box test equipment was used which has dimensions (6 x 6 x 2) cm, for determination of internal friction angles (ϕ) of sand. All tests were performed with strain controlled direct shear test machine with constant shearing rate 0.5 mm/min. (Direct shear brand was ELE)

4.2.3. Internal Friction Angle of Sand

Direct shear tests were conducted for determination of friction angle (ϕ) of sand of relative density (Dr= 10%). The sample was prepared in direct shear box and three direct shear tests were performed under three different normal stress (54.5, 109, and 163.5 kPa) according to ASTM D3080-72(1989) [44]. Table 4.3 shows the internal friction angle of the sand obtained by direct shear test corresponding to the relative density of the sand.

Table 4.3. Internal friction angle of the sand corresponding to relative density

Relative density of the sand, Dr (%)	Internal friction angle of the sand (ϕ)
10	41.0°

4.3. Features of Steel Plate

In the experiment, steel plate was put to use in the sheet-pile wall modeling. The aim to use it is to know whether the material is standard and its technical properties are known or not. Also, because of the fact that it was cut to the desired size and had the capacity to make the desired deflection in the experiment, this steel plate was put to use as a sheet-pile. In land applications cases, steel sheet-piles were also used. In the experiments. [45.] Steel plates with 2.5 mm thickness and 0.75x0.4 meters were used.

Table 4.4. Material properties of steel sheet-pile [45]

Model of Plate	Average Dry Unit Weight (γ_d), (kN/m^3)	Modulus of Elasticity of the Sheet Pile (E) (kN/m^2)	Poisson's ratio
Steel	78.5	$2*10^8$	0.30

4.4. Experiment Procedure

A model system has been constituted for the examination of the behavior of the sheet-piles in sandy soil in the experiments. The deflection of the sheet-pile and the foundation were investigated; by loading the model foundation by means of the hydraulic system, the depth of the soil behind the sheet-pile wall and by changing the distance of the foundation to the sheet-pile;. The deflection control was taken from the two ends of the foundation and from the center of the sheet-pile wall. In the study, 0.75x0.75x1 meter reservoir was used to model semi-infinite medium. With the dimensions of 12x12 cm, foundation model was used. Also steel plate with 40 cm high and 2.5 mm wall thickness was used.

According to the test standards, the loading velocity was determined to be as 1.5-2.2 mm settlement per minute in the experiments, and data recording interval is adjusted to 1 s.

Before the sheet-piles were placed in the test set, the 2 mm aluminum L profile was placed on the 2 sides to be smooth. As in Figure 4.9 after providing smoothness with a water level, these aluminum profiles are fixed to the side of the test set with the help of moving bench clamp. It was filled with a raining method from a height of 10 cm. After 50 cm of the tank was filled with sand, the sheet-pile plate was placed Figure 4.10 and the sand continued to be filled from the height of 10 cm by raining method.

Figure 4.9. L fixing the profiles

Figure 4.10. Placing the plate

When the sand filling process has been completed, the front of the sheet-pile leveled to be flat with the water level as shown in Figure 4.11.

(a)

(b)

Figure 4.11. (a) Earth leveling.1 (b) Earth leveling.2

After that the excavation of the soil behind the sheet pile for the different heights was started, leveling the earth as shown in figure 4.12 and 4.13.

(a)

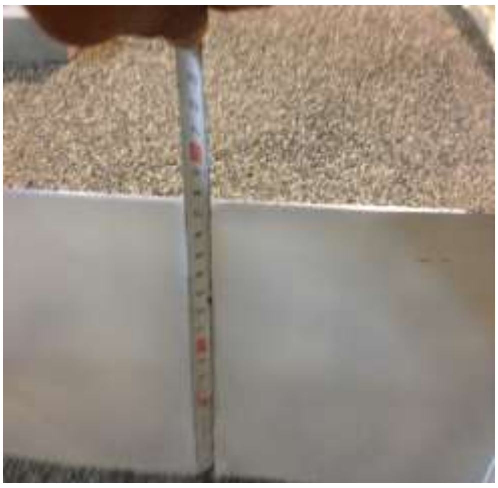

(b)

Figure 4.12. (a) Excavation of soil.1 (b) Excavation of soil. 2

(a)

(b)

Figure 4.13. (a) Excavation of soil.3 (b) Earth leveling

Therefore, as in Figure 4.14, the foundation was placed again and its leveling was checked again. After the lvdt devices were again located, the leveling of the base was checked as shown in Figure 4.15 and 4.16. If the foundation is not completely leveled and the foundation will be loaded eccentrically then the test will not be satisfying.

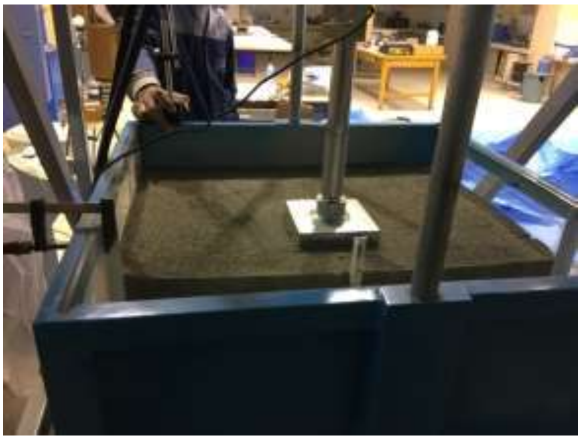

Figure 4.14. Placing the foundation

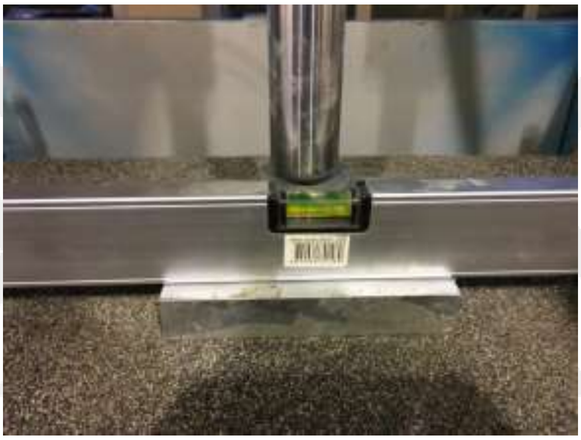

Figure 4.15. Foundation leveling control -1

Figure 4.16. Foundation leveling control -2

Setting the lvdt on the two edges of the foundation and center of the sheet pile is shown in figure 4.17.

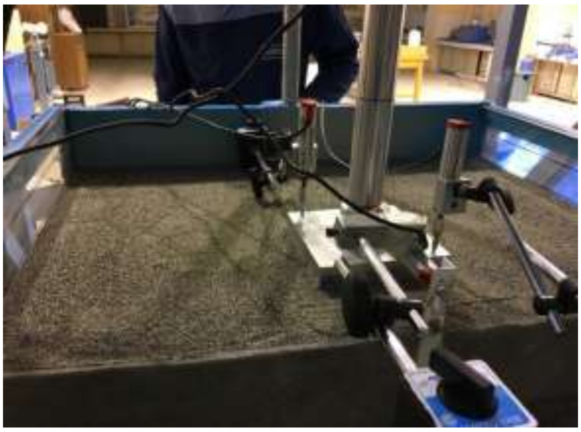

Figure 4.17. Setting the lvdt

After finishing the load and obtained all the data the lvdt devices on the foundation and sheet pile were taken out as were shown in Figure 4.18 and 4.19.

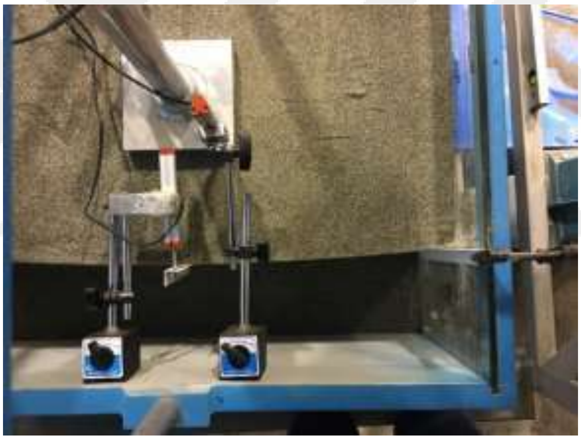

Figure 4.18. Taking out the lvdt

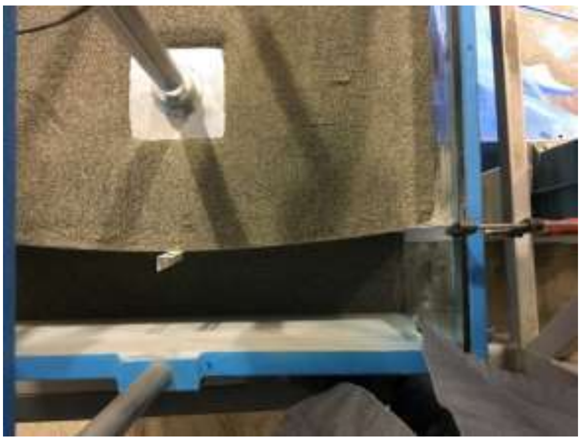

Figure 4.19. Taking out the lvdt

Figure 4.20, 4.21, 4.22 were shown the models sestem, loading of the model and cross section of the test that drawn by autocad 2D and 3D max.

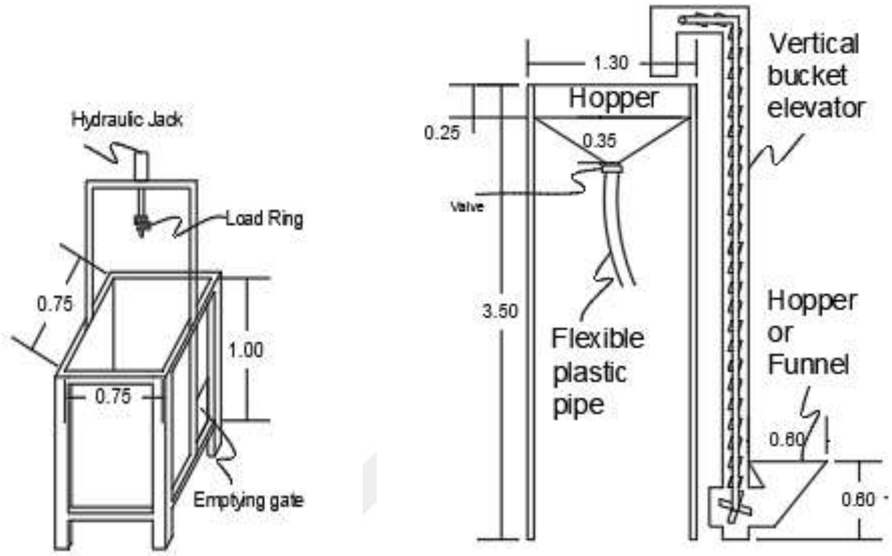

Figure 4.20. Model system

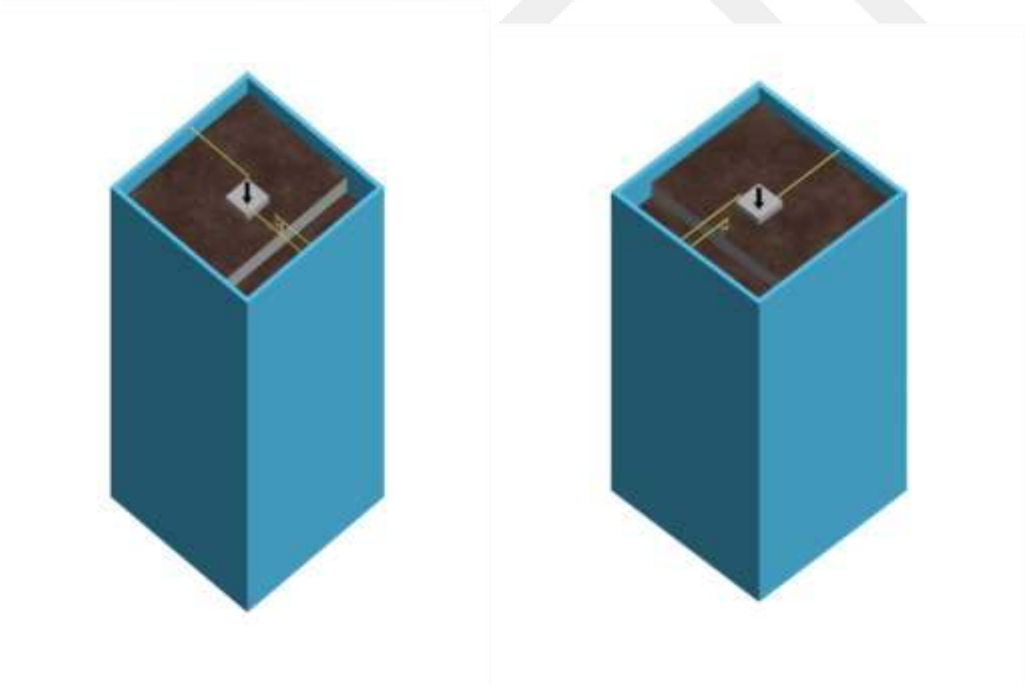

Figure 4.21. Loading of the system

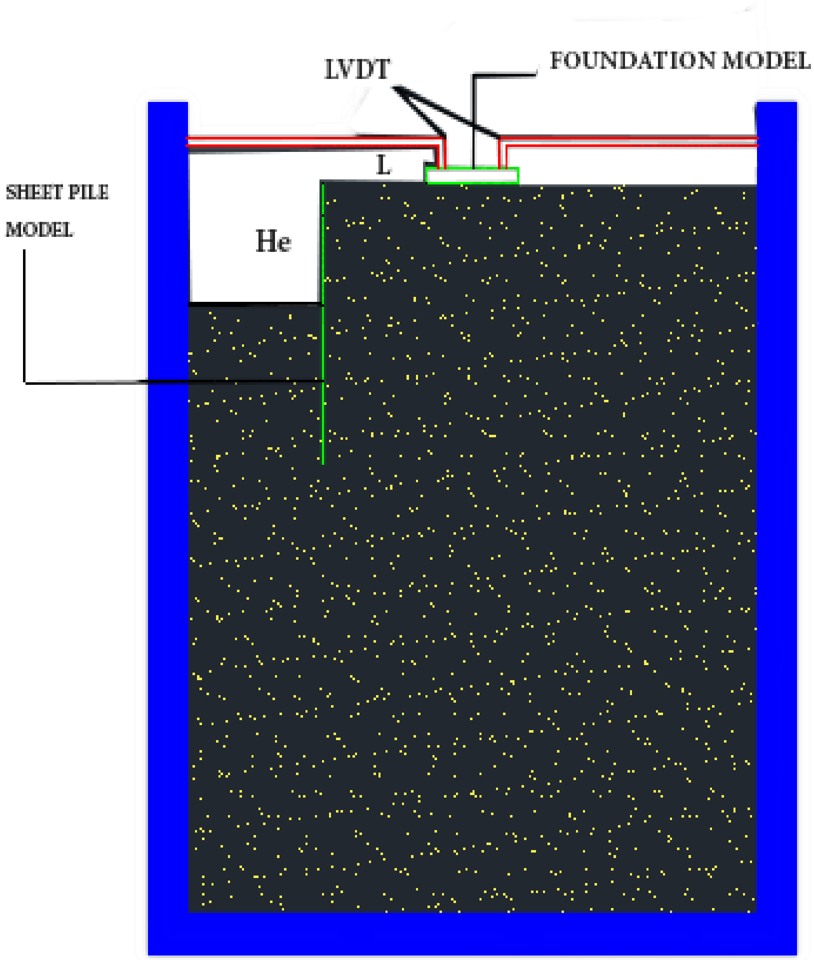

Figure 4.22. Cross section of the model

5. RESULTS

As a result of data acquired from the experiments by using various excavation depth of the soil behind the sheet-pile and foundation distances; the deflection-force graphs of the sheet-pile and the deflection-force graphs of the foundation were plotted. By comparing these graphs with each other, the effects of various excavation depth of the soil behind the sheet-piles and foundation distances were investigated.

The relative density of the sand which used in the experiments was 10%. The foundation began to be settled by the effect of load in case of 10% relative density. By this means, in the experiment, it couldn't be observed the ultimate bearing capacity and ultimate bearing capacity was supposed to be in the case when reached 12 mm deflection, which corresponds to 10% of the foundation dimension.

Ten tests were done in the laboratory of the model of foundation and sheet pile, one of them only used the foundation model without the sheet pile. The nine other were used the foundation and sheet pile for different distance between foundation and sheet pile and also different excavation depth of soil behind the sheet pile. It used three different distance between foundation and sheet pile, first distance between foundation and sheet pile was equal to length of the foundation (B=12cm), second distance was equal to (1.5B=18cm) and third distance was equal to (2B=24cm),and also it used three different excavation depth of soil behind the sheet pile, first excavation depth was equal to length of the foundation (B=12cm), second excavation depth was equal to (1.5B=18cm) and third excavation depth was equal to (2B=24cm).There were putted four pressure transducers on the sheet pile of depth of (10cm, 20cm 30cm, and 40cm) to find the lateral pressure of the soil on the sheet pile in different depth. Because of these tests it was found the settlement of the foundation, bearing capacity, deflection of the sheet pile and lateral pressure of the soil on the sheet pile. In the tables and graphs below were shown all the data of the experiments of the load, settlement of the foundation, deflection of sheet pile and lateral pressure of soil on the sheet pile. It is accepted that the failure point is in 10% of the length of the foundation means in 12mm, so all the data (load, deflection of sheet pile and lateral pressure) were taken when the settlement of the foundation was 12mm.

Comparisons of Distance between foundation and Sheet-pile:

As shown in the Figure 5.1, in the case where the distance between foundation and sheet-pile (L) was 1B, 1.5B, 2B, respectively, the excavation depth of soil behind the sheet pile (H_e) were 1B, 1.5B, 2B and the settlement of the foundation was 12 mm; as a result the deflection of the sheet-pile was obtained shown. In the Figure 5.1 and from the figure we can see when the excavation depth of soil behind the sheet pile (H_e) was increased the deflection of the sheet pile increased and when the distance between foundation and sheet pile (L) is increased the deflection of the sheet pile is decreased.

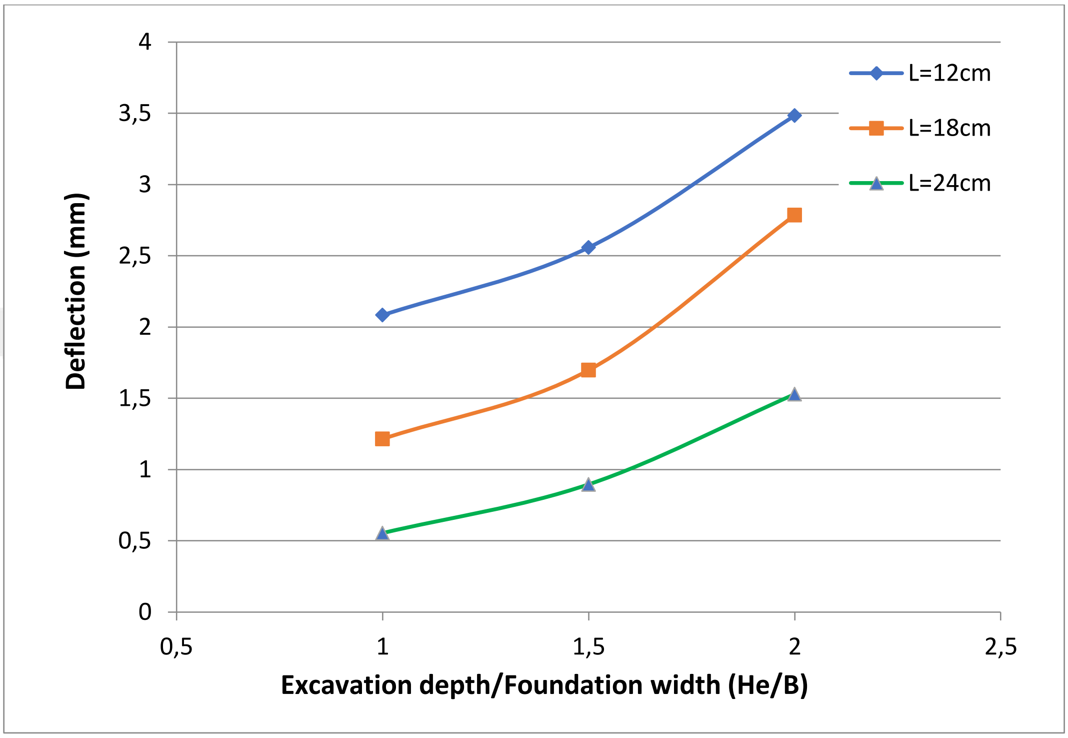

Figure 5.1. Comparisons of distance between foundation and Sheet-pile for deflection of sheet pile

Comparisons of Distance between foundation and Sheet-pile:

As shown in the Figure 5.2 in the case where the distance between foundation and sheet-pile (L) was 1B, 1.5B, 2B, respectively, the excavation depth of soil behind the sheet pile (H_e) were 1B, 1.5B, 2B and the settlement of the foundation was 12 mm; as a result the load on the foundation was obtained as shown in the Figure 5.2 and we can see from the figure when the excavation depth of soil behind the sheet pile (H_e) was increased the load capacity decreased and when the distance between foundation and sheet pile (L) was increased the load capacity decreased until the value is not changed or a small change.

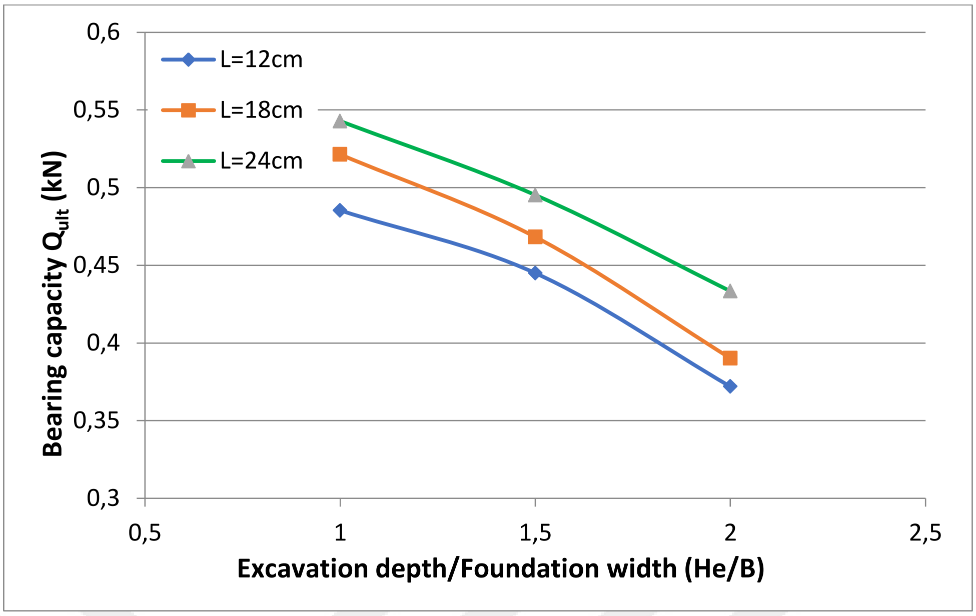

Figure 5.2. Comparisons of distance between foundation and Sheet-pile for load on the foundation

As a result of data acquired from the experiments by using various pressure transducers on the sheet-pile on the depth of 10, 20, 30, and 40 cm, and also the lateral pressure of soil on the sheet pile wall of various depth were investigated, when the distance between foundation and sheet pile were 12cm, 18cm, and 24cm as shown in the figures 5.3, 5.4, 5.5 and tables 5.1, 5.2 and 5.3.

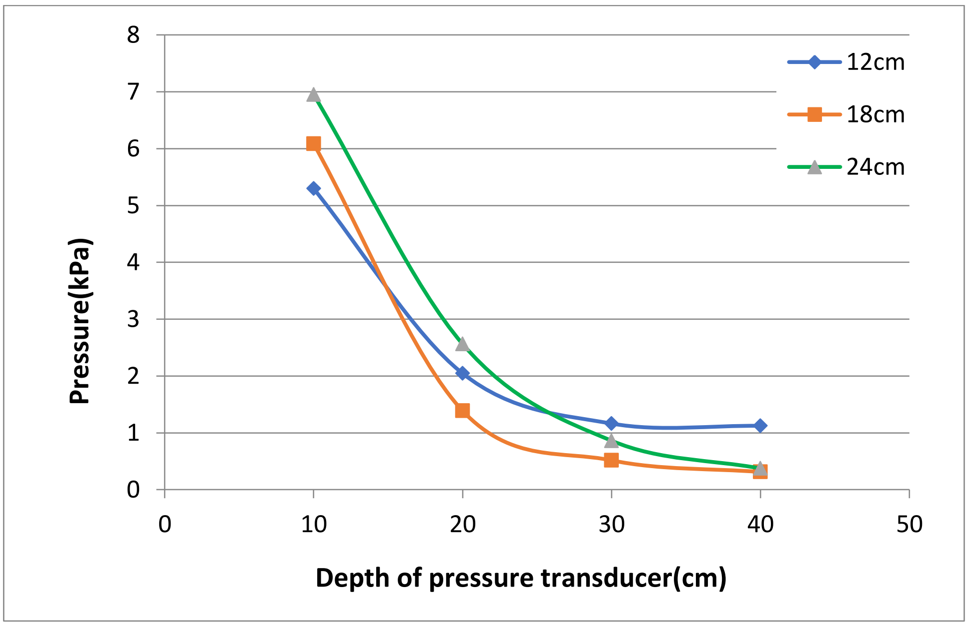

Figure 5.3. Lateral pressure on the sheet pile to various depth-L=1B

L=1B

Table 5.1. Lateral pressure on the sheet pile-L=1B

Set=12 mm	10cm	20cm	30cm	40cm
H=1B	5.297	2.0466	1.16432	1.12336
H=1.5B	6.0858	1.3888	0.5167	0.312045
H=2B	6.9503	2.5639	0.8622	0.374455

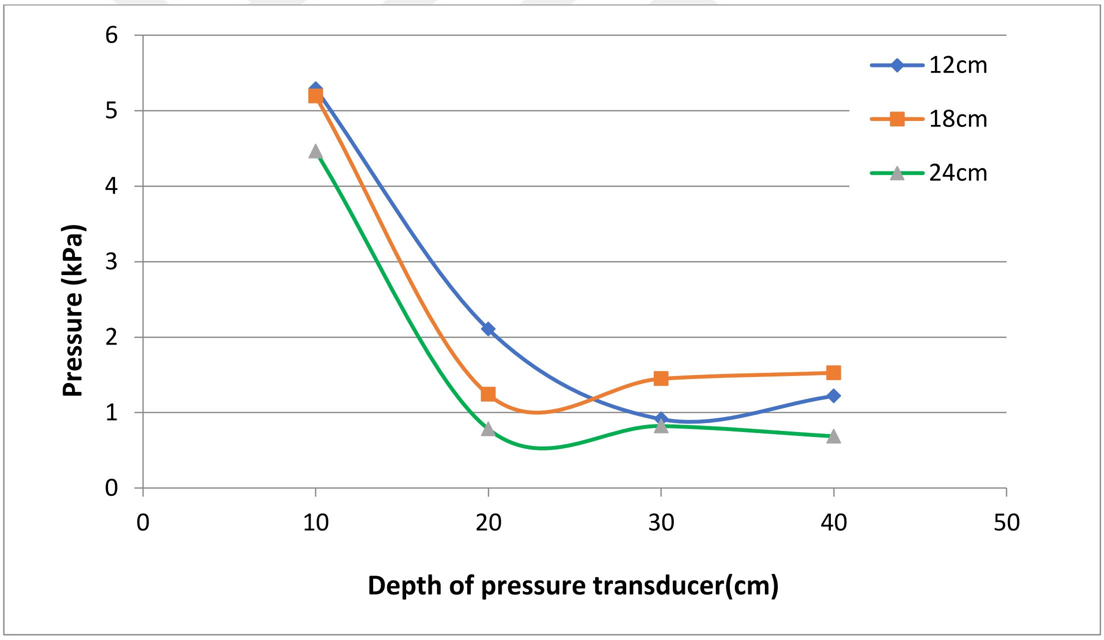

Figure 5.4. Lateral pressure on the sheet pile to various depth-L=1.5B

L=1.5B

Table 5.2. Lateral pressure on the sheet pile-L=1.5B

Set=12cm	10cm	20cm	30cm	40cm
H=1B	5.8512	1.723	1.2481	1.93
H=1.5B	7.946	1.0518	0.9565	1.3655
H=2B	6.1197	1.8197	0.7734	0.505

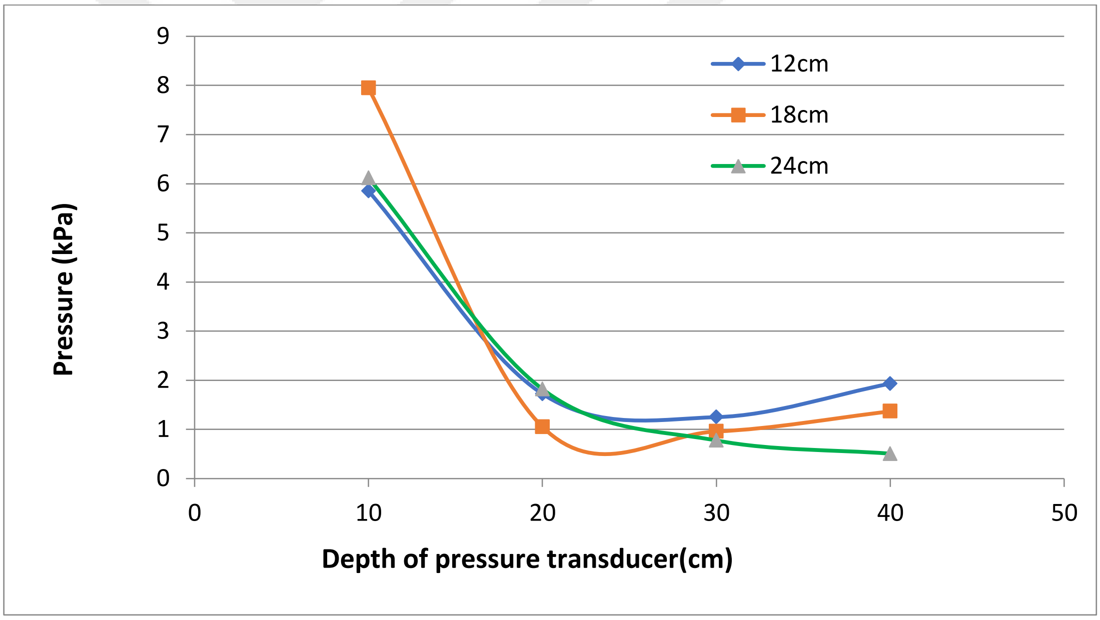

Figure 5.5. Lateral pressure on the sheet pile to various depth-L=2B

L=2B

Table 5.3. Lateral pressure on the sheet pile-L=2B

Set=12 mm	**10cm**	**20cm**	**30cm**	**40cm**
H=1B	5.29	2.1045	0.9138	1.219
H=1.5B	5.1926	1.2395	1.449	1.5269
H=2B	4.4621	0.78274	0.8224	0.6865

6. FINITE ELEMENT ANALYSIS

6.1. Introduction

Usually, the geotechnical engineering problems can be very difficult and complicated because of their boundary conditions. However, there are some simplified theories invented by some researchers can be used to solve these kinds of problems. Because of soil variability, these problems can be more complex and in this case numerical analysis can be very useful.

Numerical analysis has turn out to be extra popular in the analysis and design of geotechnical structures such as retaining walls, foundation and dams, etc. Important projects sometimes are numerically analyzed and it is also very effective in problems of soil-structures interaction.

In finite element analysis technique, the domain of the problems are meshed into a small elements which is composed of hundreds or thousands of small elements and nodes, suitable boundary conditions and proper essential models such as Mohr-Coulomb and linear elastic are applied, for all of the nodes equations are made and by solving theses equations every variables are found at the nodes.

Some people write a special finite element program for their self which can be used in solving geotechnical engineering problems. There are also some popular numerical finite element programs which are used by geotechnical engineers very often such as PLAXIS, GEO-SLOPE. Besides, there is some other software which is more powerful such as ABAQUS and ANSYS and these programs can be used in many engineering aspects such as materials, structures, concrete and also can be used in analysis of geotechnical engineering problems. Those two programs are also utilized in many universities they are effective for teaching and research purposes.

6.2. Plaxis 3D Program

PLAXIS 3D is the most popular graphical user interface geotechnical program which is based on the finite element analysis and very often used by geotechnical engineers especially in modeling and analysis of soil-structure interaction such as foundation, retaining walls, soil slope stability, etc. The program has been designed in a way that the user can easily model any soil-structure interaction problems and study the behavior of the structure under loading.

Recently, many researchers use finite element technique for analysis and study soil-structure interaction problems. In this study, finite element analysis has been conducted by

PLAXIS 3D software package. The model (foundation and sheet pile) are modeled and axial load applied to the foundation so the results were obtained in term of settlement versus bearing capacity of the foundation and also deflection of the sheet pile and the finite element results were compared to the experimental results.

6.3. Model Foundation and Sheet Pile Analysis

In this study the numerical finite element software PLAXIS 3D has been used for analysis of foundation and sheet pile model. The Mohr-Coulomb failure criteria were used to conduct finite element analysis and the dry condition was considered for the model sand. The totally ten model foundations and sheet pile load tests were analyzed with only one relative density of the sand mentioned in this study before. In each test the results obtained in term of sheet pile deflection versus axial load and foundation displacement versus axial load.

6.3.1. Boundary Conditions

In analysis of model foundation and sheet piles in Plaxis 3D "Standard Fixities" has defined for the boundary condition which is made automatically by the software. Furthermore, rigid interfaces were defined, that means, there is no relative movement between the nodes of the finite elements which represent the model foundation and sheet pile and those of the finite elements which represent the ground soil. In the three-dimensional analysis, 15-node wedge elements are generally used. The schematic representation of the 15-node elements used in the analysis is shown in Figure 6.1

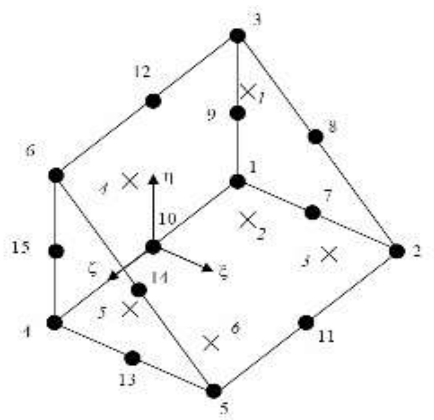

Figure 6.1. Node Wedge Elements in 3D Analysis (Plaxis 3D Foundation Tutorial Manual, 2007)

Nodes (●) and strain points (x)

6.3.2. The Mesh Generation

In Plaxis 3D, a two-dimensional top-view mesh is generated first, after that the three-dimensional mesh is generated with the standard procedure of the software. Figure 6.2 shows the two and three dimensional mesh generated in the program.

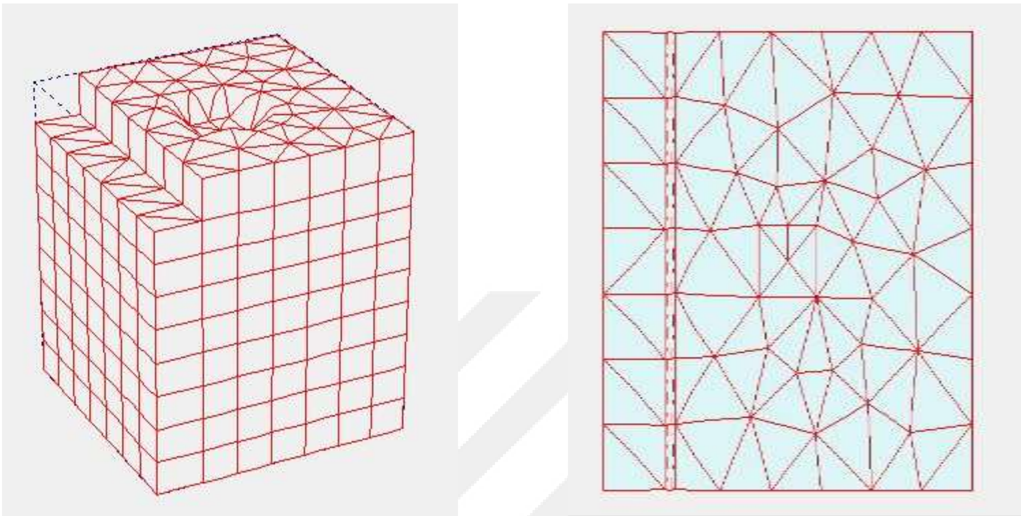

Figure 6.2. 2D and 3D dimensional mesh generated in plaxis 3D program

6.4. The Material Parameters Used in the Analysis

The sand was modeled to meet the Mohr-Coulomb failure criterion under drained conditions, the dry unit weight of the sand corresponding to relative density was input to the Plaxis 3D. The model foundation and sheet piles were modeled to meet the linear elastic and non-porous and their unit weight also were given to Plaxis 3D program. Table 6.1, and 6.2 shows the parameters of the sand, foundation and sheet pile materials used in Plaxis 3D.

Table 6.1. The parameters of the sand used in plaxis 3D program

Relative Density (Dr, %)	Average Dry Unit Weight (γ_d), (kN/m^3)	Modulus of Elasticity of the Sand (E) (kN/m^2)	Poisson's ratio	Internal friction angle of the sand (ϕ)(°)	Dilatancy angle of the sand (ψ)(°)	R_{int}	Cohesion (kN/m^2)
10	14.6	500	0.15	41	11	0.67	0.4

Table 6.2. The parameters of the model foundation and sheet piles used in plaxis 3D program [45]

Model	Average Dry Unit Weight (γ_d), (kN/m^3)	Modulus of Elasticity of the Piles (E) (kN/m^2)	Poisson's ratio
Foundation	78.5	$2*10^8$	0.3
Sheet pile	78.5	$2*10^8$	0.3

6.5. Results from Finite Element Program

After the sand and model foundation and sheet piles were modeled in the Plaxis 3D, the total bearing capacity chosen from the experimental load-settlement, the same load value applied to the foundation and sheet pile in Plaxis 3D by using the parameters mentioned above. The results showed that there is a good agreement of the Plaxis 3D finite element program compared to the experimental results. The data were given in Figure 6.3 and Figure 6.4.

Comparisons of Distance between foundation and Sheet-pile

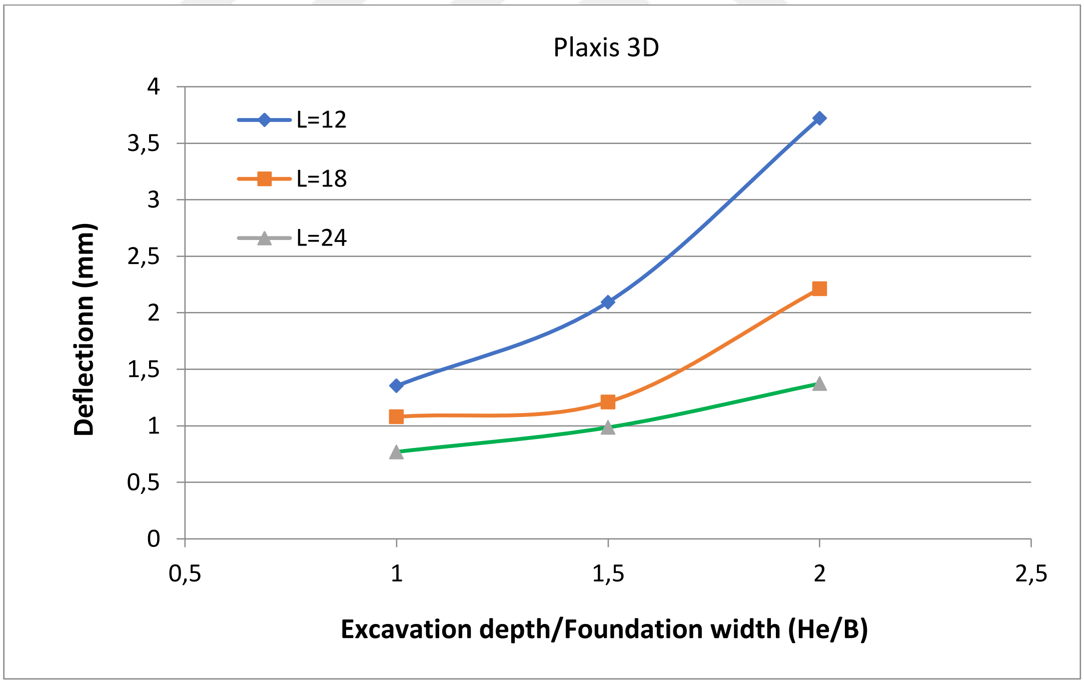

Figure 6.3. Comparisons of distance between foundation and sheet-pile for deflection of sheet pile

Comparisons of Distance between foundation and Sheet-pile

Figure 6.4 show the Plaxis 3D finite element program for bearing capacity Qult (kN)

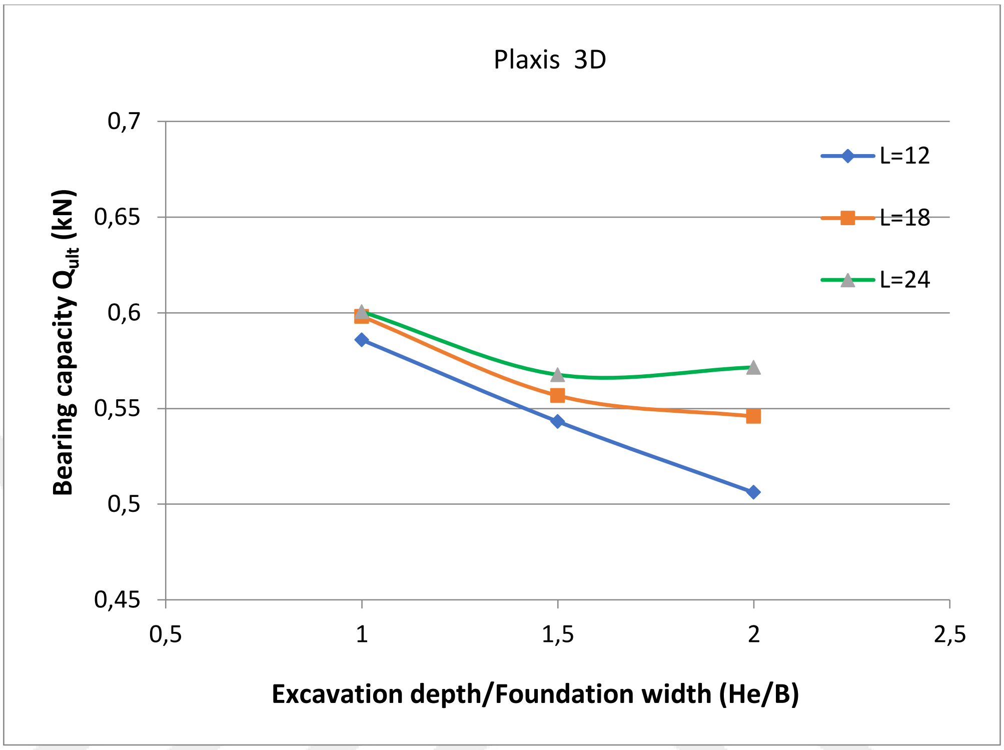

Figure 6.4. Comparisons of distance between foundation and sheet-pile for load on the foundation

To get a better view and easily compare the results of the experimental tests with results achieved from Plaxis 3D finite element, the results from experimental and Plaxis 3D combined in a graphical figure next to each other. The graphical comparisons between experimental results with Plaxis 3D results are shown in Figures 6.5 and 6.6 that shows the deflection of the sheet pile, and Figures 6.7 and 6.8 shows the bearing capacity-displacement curves of the model foundation analysis.

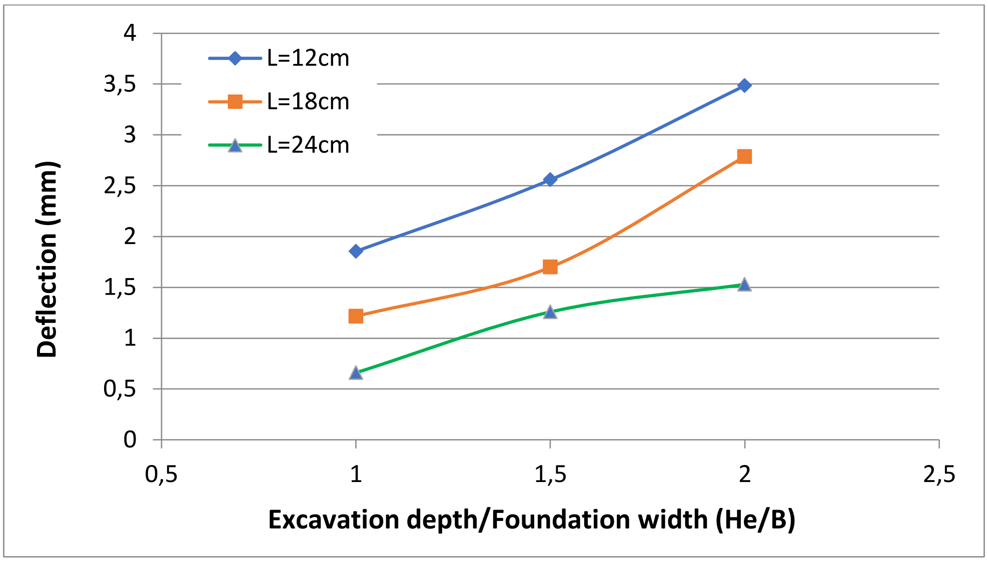

Figure 6.5. Experimental study

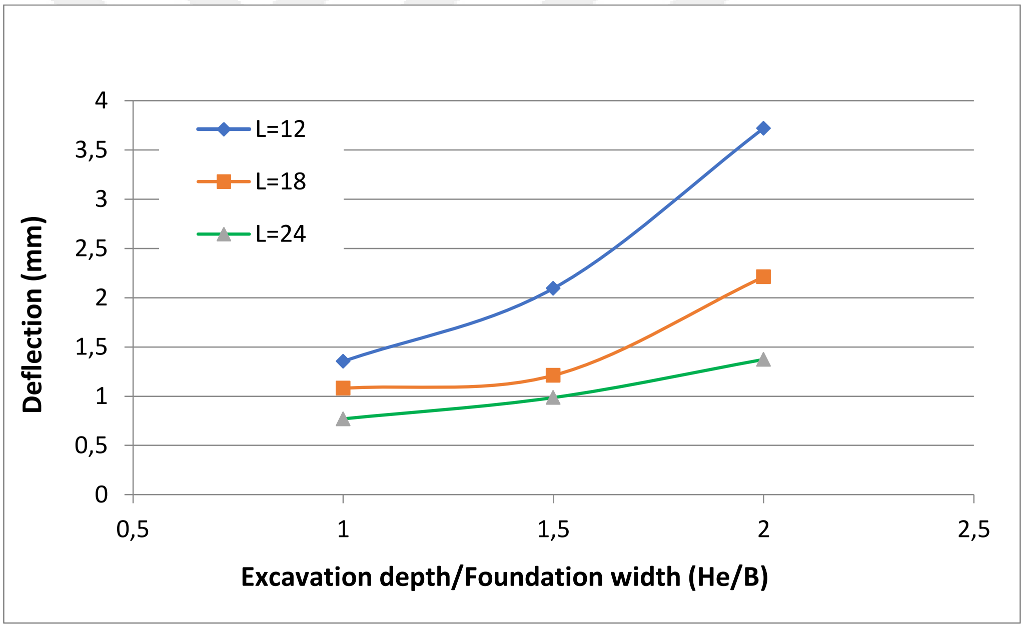

Figure 6.6. Plaxis 3D

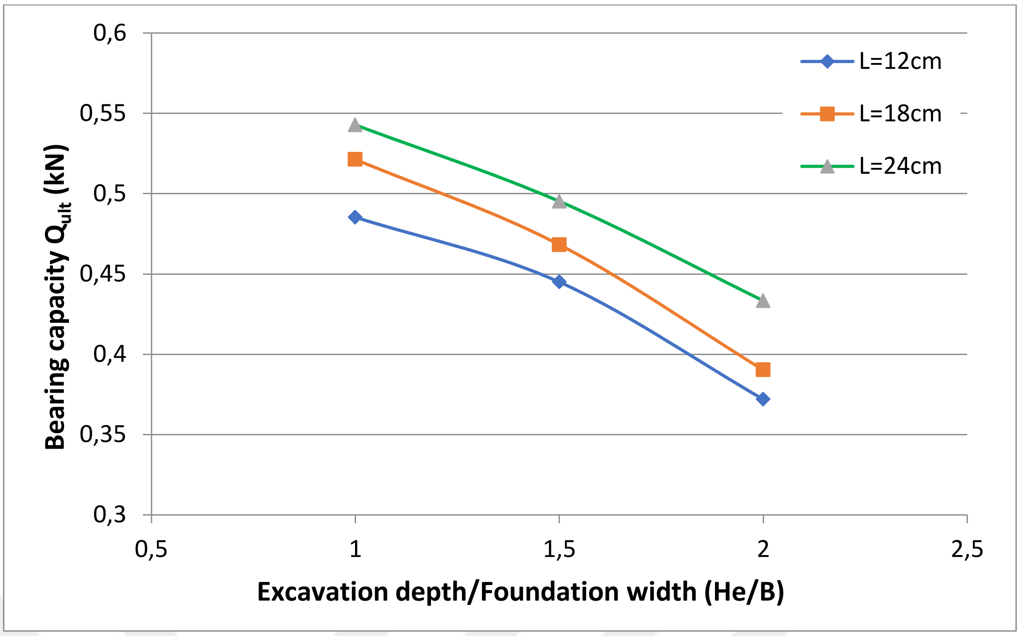

Figure 6.7. Experimental study

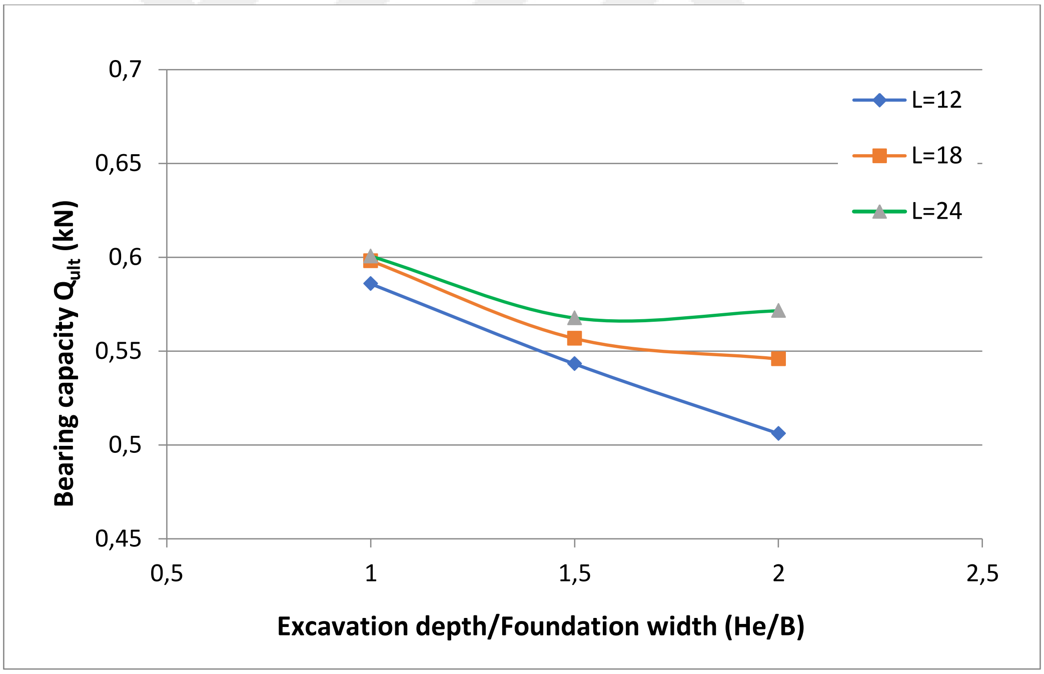

Figure 6.8. Plaxis 3D

In the Figure 6.9 shows the comparison between experimental study and Plaxis 3D

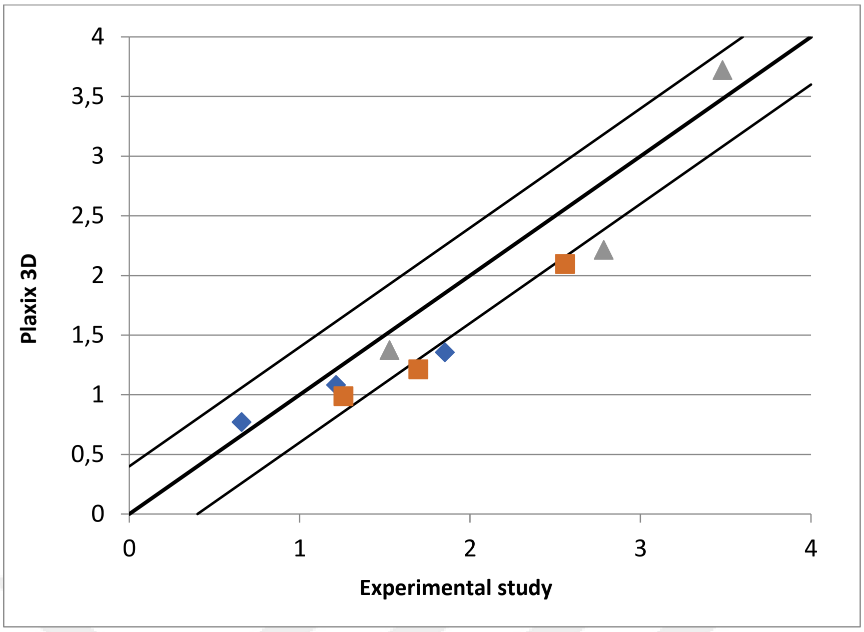

Figure 6.9. Comparison of deflection between experimental study and plaxis 3D

Some of Plaxis 3D figures 6.10 and 6.11 that shown 3D meshes of the model

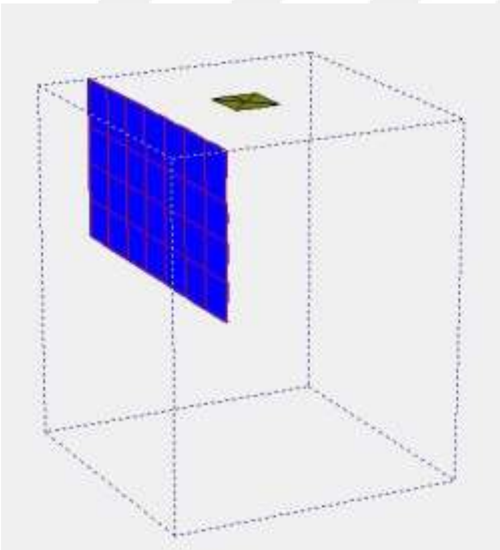

(a)

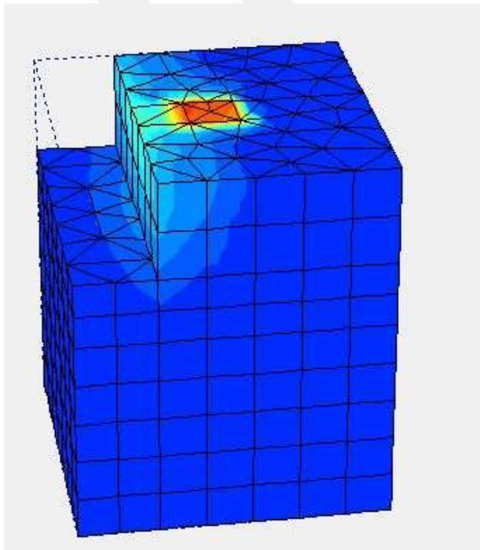

(b)

Figure 6.10. (a) Model plaxis 3D (b) Typical displacement plaxis 3D

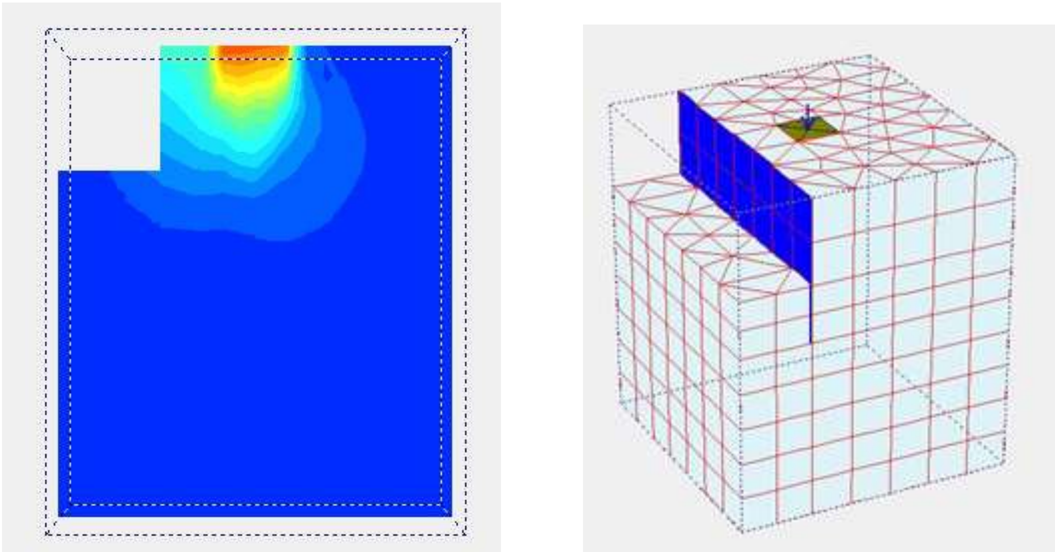

(a) (b)

Figure 6.11. (a) Typical vertical displacement (b) 3D mesh generated

7. STATISTICAL ANALYSIS OF LATERAL PRESSURE

Multiple regression analysis was used to estimate lateral pressures. Statistical analysis includes the use of statistical data involving different factors, individuals and events to quantitatively assess probabilistic or statistical relationships. In this chapter the estimated lateral pressures were measured and comparison between the experimental study and the estimated lateral pressure analysis were done, as well as the frequency histogram curves for all results.

Mean: Most people commonly refer to the mean as the average. The average refers to the number that you get by adding a set of numbers and dividing the sum by the set's total number. The mean is also more accurately called the arithmetic mean.

$$\text{Mean } (\mu) = \frac{sum\ of\ elements\ in\ set}{number\ of\ elements\ in\ set}$$

Maximum: is the maximum value in set.

Minimum: is the minimum value in set.

Standard deviation: a statistic that measures a data set's dispersion relative to its mean. It is calculated as the square root of the variance by measuring the difference in mean between the data points. It is calculated as the square root of the variance If the data points are farther from the mean, the variance within the dataset is greater; thus, the more data is distributed, the higher the standard deviation

The formula for standard deviation (SD) is: $\text{SD} = \sqrt{\frac{\sum|\boldsymbol{x}-\mu|^2}{\boldsymbol{N}}}$

Where $\sum$ means "sum of", x is a value in the data set, μ is the mean of the data set, and N is the number of data points in the set.

Skewness: This is the degree of the symmetrical bell curve distortion or normal distribution. This tests the data distribution's lack of symmetry. It is distinguishes from one tail to other extreme values. The skew of a symmetric distribution is 0.

There are two types of Skewness: Positive and Negative.

Positive Skewness: Means when the tail is shorter and fatter on the right side of the distribution. The mean and median will be greater than the mode.

Negative Skewness: Means when the tail is shorter and fatter on the right side of the distribution. The mean and median will be greater than the mode.

Kurtosis: Kurtosis is about the distribution's tails and not the peaks or hovers. With respect to the other tail, the extreme values are described in one. It is also the estimate of the outer part of the distribution.

Table 7.1 shows the determination of the parameters of statical analyses for all the data.

Table 7.1. Descriptive statistical parameters of the samples

	z	L	He/B	z/L	α	Ds
Mean	25	18	1.5	1.50463	43.74441	2.37957
Minimum	10	12	1	0.41667	18.43495	0.31205
Maximum	40	24	2	3.33333	65.77225	7.946
Std.Dev	11.33893	4.96847	0.41404	0.83499	14.74846	2.18159
Skewness	0	0	0	0.726298	-0.302752	1.231999
Kurtosis	-1.38253	-1.54412	-1.54412	-0.11879	-1.07585	0.12146
Valid N	36	36	36	36	36	36

Table 7-2. Coefficients of variables

A	C	D	E	F	G	H
-7503.93	0.1	0.02	5.37	-0.89	0.2	7510.57

$$\Delta\sigma = e^{A.z^{0.01} + C.z + D.L^{1.5} + E.\left(\frac{He}{B}\right)^{0.01} + F.\left(\frac{z}{L}\right) + G.\alpha + H} \tag{7.1}$$

$$\alpha = \tan^{-1} \frac{z}{L+\frac{B}{2}} \tag{7.2}$$

By the equation (7.1) the estimated data calculated. Table 7.3 shows the used dataset in the statistical analyses. Figure 7.1 and Figure 7.2 shows the frequency histogram for all data and comparison between experimental study and estimated study for lateral pressure.

Table 7.3. Used dataset in the statistical analyses.

z	L	He/B	z/L	α	Ds
10	12	1	0.833333333	29.0546041	5.297
20	12	1	1.666666667	48.0127875	2.0466
30	12	1	2.5	59.03624347	1.16432
40	12	1	3.333333333	65.77225468	1.12336
10	12	1.5	0.833333333	29.0546041	6.0858
20	12	1.5	1.666666667	48.0127875	1.3888
30	12	1.5	2.5	59.03624347	0.5167
40	12	1.5	3.333333333	65.77225468	0.312045
10	12	2	0.833333333	29.0546041	6.9503
20	12	2	1.666666667	48.0127875	2.5639
30	12	2	2.5	59.03624347	0.8622
40	12	2	3.333333333	65.77225468	0.374455
10	18	1	0.555555556	22.61986495	5.29
20	18	1	1.111111111	39.80557109	2.1045
30	18	1	1.666666667	51.34019175	0.9138
40	18	1	2.222222222	59.03624347	1.219
10	18	1.5	0.555555556	22.61986495	5.1926
20	18	1.5	1.111111111	39.80557109	1.2395
30	18	1.5	1.666666667	51.34019175	1.449
40	18	1.5	2.222222222	59.03624347	1.5269
10	18	2	0.555555556	22.61986495	4.4621
20	18	2	1.111111111	39.80557109	0.78274
30	18	2	1.666666667	51.34019175	0.8224
40	18	2	2.222222222	59.03624347	0.6865
10	24	1	0.416666667	18.43494882	5.8512
20	24	1	0.833333333	33.69006753	1.723
30	24	1	1.25	45	1.2481
40	24	1	1.666666667	53.13010235	1.93
10	24	1.5	0.416666667	18.43494882	7.946
20	24	1.5	0.833333333	33.69006753	1.0518
30	24	1.5	1.25	45	0.9565
40	24	1.5	1.666666667	53.13010235	1.3655
10	24	2	0.416666667	18.43494882	6.1197
20	24	2	0.833333333	33.69006753	1.8197
30	24	2	1.25	45	0.7734
40	24	2	1.666666667	53.13010235	0.505

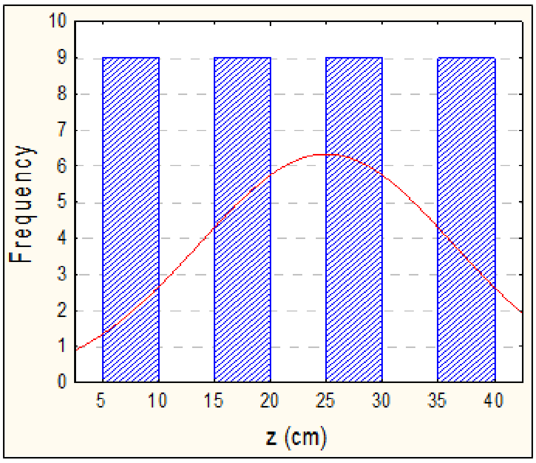

(a)

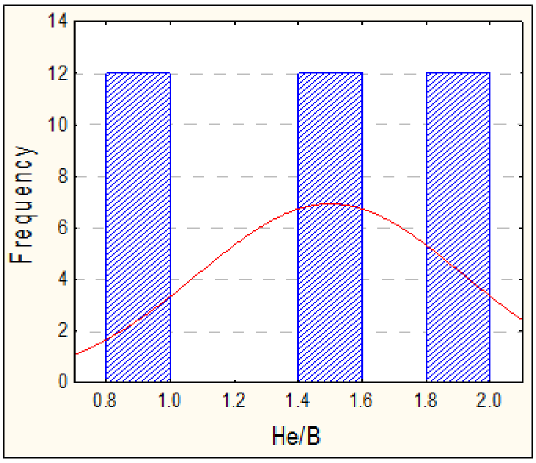

(b)

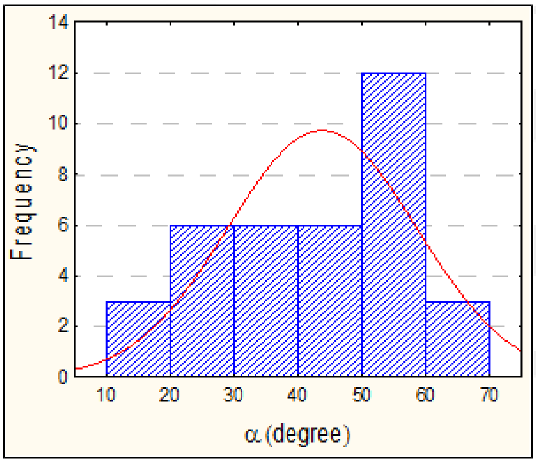

(c)

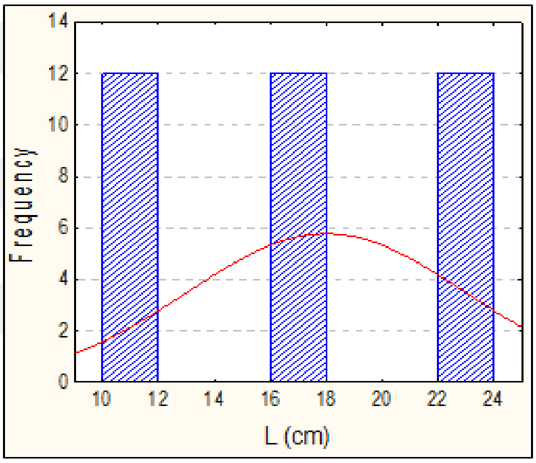

(d)

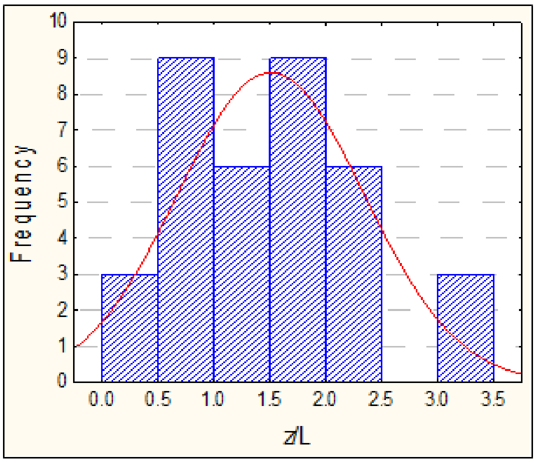

(e)

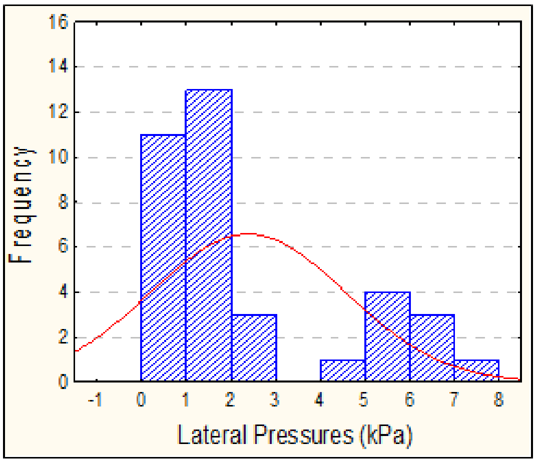

(f)

Figure 7.1. (a), (b), (c), (d), (e), (f) Frequency histogram of test results

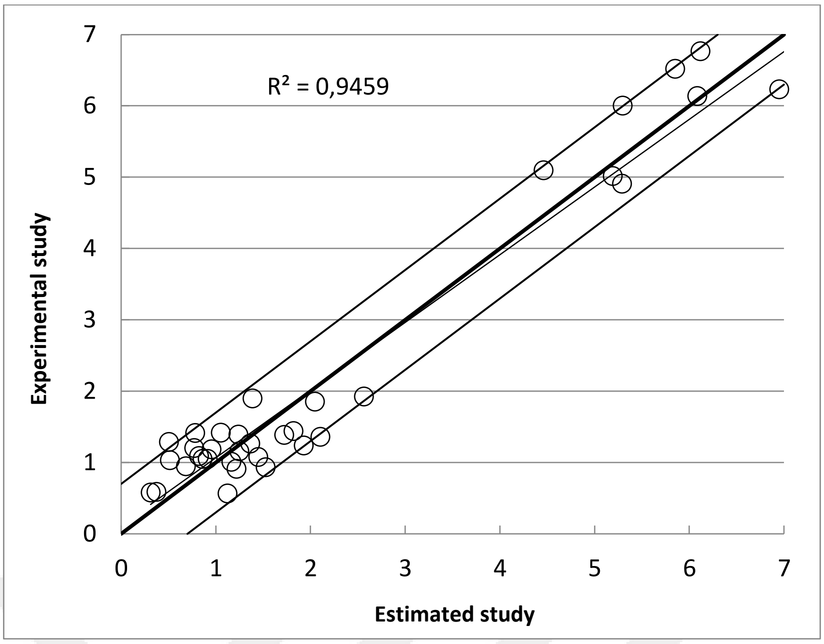

(a)

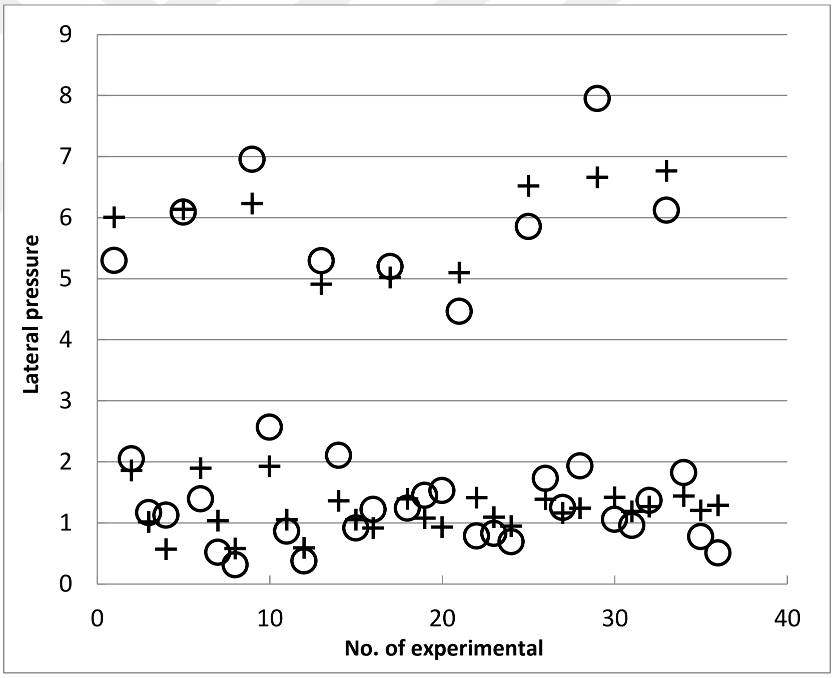

(b)

Figure 7.2. (a), (b) Comparison of experimental data with estimated data.

8. CONCLUCISIONS

Direct shear tests were performed to estimate the internal friction angle of the sand for relative densities 10%. The direct shear test was done under three different normal stresses with constant shearing rate 0.5 mm/min. The interaction behavior between steel foundation model and steel sheet pile wall was investigated using experimental analysis and finite element analysis, finite element program Plaxis 3D was also used to study the behavior of same model sheet pile and model foundation under axial loading. The analysis was made with different distance between foundation and sheet pile and different excavation depth of soil behind the sheet pile, three different distances between foundation and sheet pile and three different excavation depth of soil behind the sheet pile. The response variables analyzed included foundation settlement, deflection of sheet pile, Bearing capacity Qult and lateral pressure of soil on the sheet pile. The following conclusions achieved from the test results.

- From the distance between foundation and sheet pile, it was found that when the distance was increased the deflection of the sheet pile decreased for the same excavation depth and when the distance was increased the load capacity on the foundation is increased for the same excavation depth.
- From the experimental study, it was found that when the excavation depth was increased the deflection of the sheet pile increased for the same distance between foundation and sheet pile and when the excavation depth was increased the load capacity decreased for the same distance between foundation and sheet pile.
- From the finite element analysis like the experimental results the load capacity of the model foundation increases with increasing distance between foundation and sheet pile and load capacity decreases with increasing excavation depth of soil behind the sheet pile. Also same behavior was observed for the deflection of the sheet pile, the deflection of the sheet pile decreases with increasing L distance and deflection of the sheet pile increases with increasing H_e depth. The most effective parameters on the settlement behavior are the modulus of elasticity and the unit weight of the soil. The load-settlement curves achieved from the Plaxis 3D program are nearly the same which achieved from the experimental study. At the same time the load-deflection curve achieved from the Plaxis 3D program is nearly the same from the experimental load-deflection curves.
- Lateral pressures measured by using pressure transducers. These pressures analysed statistically to derive a relation between test systems geometrical conditions and measured lateral pressures. An appropirate correlation (R^2=0.95) has been determined.

- In the future, sheet piles which are placed in soils with different relative densities can be investigated.

REFRENCES

[1] Zekri, A., Ghalandarzadeh, A., Ghasemi, P., & Aminfar, M. H. (2015). Experimental study of remediation measures of anchored sheet pile quay walls using soil compaction. *Ocean Engineering,* 93, 45-63.

[2] Cherubini, C. (1997). Data and considerations on the variability of geotechnical properties of soils. *In Proceedings of the Int. Conf. on Safety and Reliability (ESREL)* (Vol. 97, No. 2, pp. 1583-1591).

[3] Cherubini C, Giasi CI, Rethati L. (1993). the coefficients of variation of some geotechnical parameters. In: Li, Lo, editors. *Proceedings of the Conference on Probabilistic Methods in Geotechnical Engineering. Canberra*. pp. 179–83.

[4] Kamran M. Nemati. (2007). University of Washington. Temporary structures. *lesson4: Cofferdams,* p 1-13..

[5] Eskandari, Leila, and Behzad Kalantari. (2011). "Basic types of sheet pile walls and their application in the construction industry—*a review." EJGE*: 1533-1541.

[6] Bao CG, Huang WF, Chang QN. (1993). Reliability analysis of bearing capacity for a gravity wharf foundation in random field theory. *In: Proceedings of the Conference on Probabilistic Methods in Geotechnical Engineering, Canberra*. p. 291–294.

[7] Young Tan, Ye Lu. (2009). Parametric Studies of DDC induced Deflections of Sheet pile Walls. *"Computers and Geotechnics*; *36(5)* pp. 902-910.

[8] Braja-M-Das (2007).*Principles-of-Foundation-Engineering*.Solution-Manual-6th-Ed.

[9] Stanislav S. (2006). Interactional Approach of Cantilever Pile Walls Analysis. *ACTA Geotechnica Slovenica*; P 47-59.

[10] Liu, L., & Dobry, R., (1997). Seismic response of shallow foundation on liquefiable sand. *Journal of geotechnical and geoenvironmental engineering*, 123(6), 557-567.

[11] Leung, C.F., Chow, Y.K., Shen, R.F. (2000). Behaviour of pile subject to excavation induced soil movement. *J. Geotech. Geoenviron. Eng*. 126 (11), 947–954.

[12] Ong, D.E.L., Leung, C.E., Chow, Y.K. (2006). Pile behaviour due to excavation-induced soil movement in clay I: Stable wall. *J. Geotech. Geoenviron. Eng*. 132 (1), 36–44.

[13] O'Rouke, T.D. (1981). Ground movements caused by braced excavation. *J. Geotech. Geoenviron. Eng.* 107 (9), 1159–1178.

[14] Guo, W.D., Ghee, E.H. (2006). Behavior of axially loaded pile groups subjected to lateral soil movement. In: Foundation Analysis and Design, Innovative Methods. *Proceedings of Sessions of GeoShanghai, Shanghai, China,* pp. 174–181.

[15] Nishanthan, R., Liyanapathirana, D.S., Leo, C. (2014). Modelling issues in simulation of deep excavations. *Aust. Geomech. J.* 49 (1), 91–103.

[16] Poulos, H.G., Chen, L.T. (1996). Pile response due to unsupported excavation-induced lateral soil movement. *Can. Geotech. J*. 33 (4), 670–677.

[17] Poulos, H.G., Chen, L.T. (1997). Pile response due to excavation-induced lateral soil movement. *J. Geotech. Geoenviron. Eng*. 123 (2), 94–99.

[18] Chen, L.T., Poulos, H.G. (1996). Some aspects of pile response near an excavation. *In:*

Proceedings, 7th Australia New Zealand Conference on Geomechanics: Geomechanics in a Changing World, Barton, ACT: Institution of Engineers, Australia, and pp. 604–609.

[19] Stewart, D. P., Jewell, R. J., and Randolph, M. F. (1994). ‘‘Centrifuge modelling of piled bridge abutments on soft ground.’’ *Soils and Found. Tokyo*, 34(1), 41-51.

[20] Torrabadella, A. G., GARCÍA-TORNEL, A. J., & PASTALLE, S. O. (2013). *Numerical analysis of cantilever and anchored sheet pile walls at failures and comparison with classical methods*. Escola de Camins.

[21] Morgenstern, N. R., & Eisenstein, Z. (1970). Methods of estimating lateral loads and deflections. *In Lateral Stresses in the Ground and Design of Earth-Retaining Structures* (pp. 51-102). ASCE.

[22] Das, B. (2011). *Principles of Foundation Engineering*. Cengage Learning, USA.

[23] Kohama, E., Sugano, T., Shiozaki, Y., Masaaki, M. (2004). Dynamic behavior of a steel sheet pile quay wall in the full scale experiment with regard to liquefaction. *In: Proceedings of the 13th World Conference on Earthquake Engineering. Vancouver, B.C., Canada*.pp no 3485

[24] Miao, L. F., Goh, A. T. C., Wong, K. S., & Teh, C. I. (2006). Three-dimensional finite element analyses of passive pile behaviour. *International Journal for Numerical and Analytical Methods in Geomechanics,* 30(7), 599-613.

[25] Hunt, Roy E. (2005), Kim, S. B., & Park, D. H. (2003). Theoretical study on flexural stiffness of innovative prestressed wale. *In Proceedings of the KSCE annual conference*. (pp. 3754–3759).

[26] Kim, N. K., Park, J. S., Oh, H. J., Han, M. Y., Kim, M. Y., & Kim, S. B. (2007). Performance of IPS earth retention system in soft clay. *Journal of the Korean Geotechnical Society*, 23(3), 5–13.

[27] Sagaseta, C. (1987). Analysis of undrained soil deflection due to ground loss.*Geotechnique* 37 (3), 301–320.

[28] Xu, K. J., & Poulos, H. G. (2000). Theoretical study of pile behaviour induced by a soil cut. *In ISRM International Symposium. International Society for Rock Mechanics and Rock Engineering.*

[29] Zhang, R., Zheng, J., Pu, H., Zhang, L., (2011). Analysis of excavation-induced responses of loaded pile foundations considering unloading effect. Tunnelling Underground Space Technol. 26 (2), 320–335.

[30] Park, R., & Paulay, T. (1975). *Reinforced concrete structures*. John Wiley & Sons.

[31] Potts, D. M. (1999). *Finite Element Analysis in Geotechnical Engineering*. Thomas Telford, London.

[32] Poulos, H.G. (2005). The influence of construction side effects on existing piles foundations. *Geotech. Eng*. 36 (1), 51–68.

[33] Ou CY, Chiou D, Wu T. (1996). Three-dimensional finite element analysis of deep excavations. *J Geotech Eng*; 122:337–345.

[34] Ou, C. Y., Shiau, B. Y., & Wang, I. W. (2000). Three-dimensional deflection behavior of the Taipei National Enterprise Center (TNEC) excavation case history. *Canadian Geotechnical Journal,* 37(2), 438-448.

[35] Nikolinakou, M. A., Whittle, A. J., Savidis, S., & Schran, U. (2011). Prediction and interpretation of the performance of a deep excavation in Berlin sand. *Journal of Geotechnical and Geoenvironmental Engineering,* 137(11), 1047-1061.

[36] Roboski, J. F. (2004). *Three-dimensional performance and analyses of deep excavations*. (Doctoral dissertation, Northwestern University).

[37] Chen, R. P., Li, Z. C., Chen, Y. M., Ou, C. Y., Hu, Q., & Rao, M. (2013). Failure investigation at a collapsed deep excavation in very sensitive organic soft clay. *Journal of Performance of Constructed Facilities,* 29(3), 04014078.

[38] Li, M. G., Zhang, Z. J., Chen, J. J., Wang, J. H., & Xu, A. J. (2017).Zoned and staged construction of an underground complex in Shanghai soft clay. *Tunnelling and Underground Space Technology,* 67, 187–200.

[39] Jianhang, L. (1999). The Theory and its Practice by Using the Rule of Time-Space Effect in Soft Soil Excavation *[J]. Undergrourd Engineering and Tunmels*, 3.

[40] Liu, A. H., Li, H., & Luo, R. W. (2010). Application of the space-time effect theory in the soft-soil foundation construction. *Chinese Journal of Underground Space and Engineering*, 6(3), 571–576.

[41] ASTM D422-63, (2007). *Standard Test Method for Particle-Size Analysis of Soils*. American Test Methods Standards, West Conshohocken, PA.

[42] ASTM D854-14. (2014). *Standard Test Methods for Specific Gravity of Soil Solids by Water Pycnometer,* American Test Methods Standards, West Conshohocken, PA.

[43] ASTM D4254-16. (2016). *Standard Test Methods for Minimum Index Density, and Unit Weight of Soils and Calculation of Relative Density*. American Test Methods Standards, West Conshohocken, PA.

[44] ASTM D3080/D3080M-11. (2011). *Standard test method for direct shear test of soils under consolidated drained conditions.* ASTM International, West Conshohocken, PA, USA.

[45] Smith, B. H., et al. (2012). "Steel foam for structures: A review of applications, manufacturing and material properties." *Journal of Constructional Steel Research* 71: 1-10.

APPENDIX

APP-1: EXPERIMENTAL LOAD-SETTLEMENT AND TIME-SETTLEMENT CURVES OF TOTAL BEARING CAPACITY OF STEEL FOUNDATION MODEL.

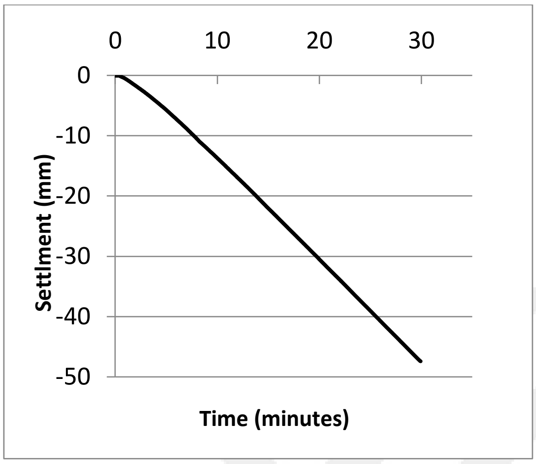

App 1.1 Time-settlement behavior (L=1B, He=1B)

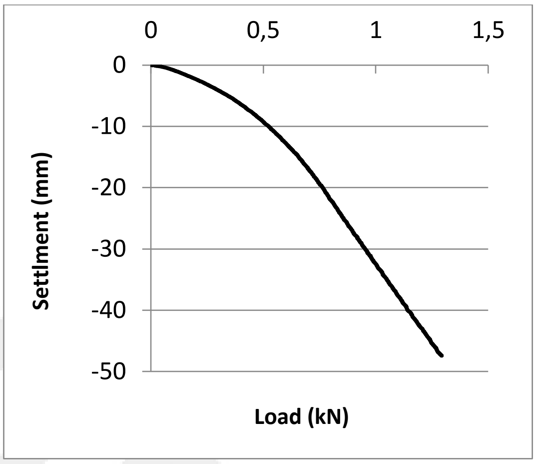

App 1.2 Load-settlement behavior (L=1B, He=1B)

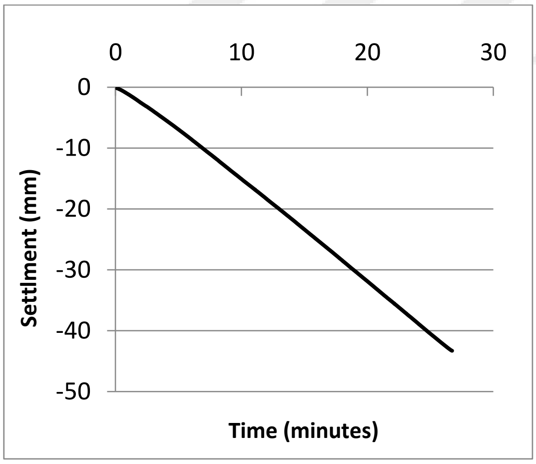

App 1.3 Time-settlement behavior (L=1B, He=1.5B)

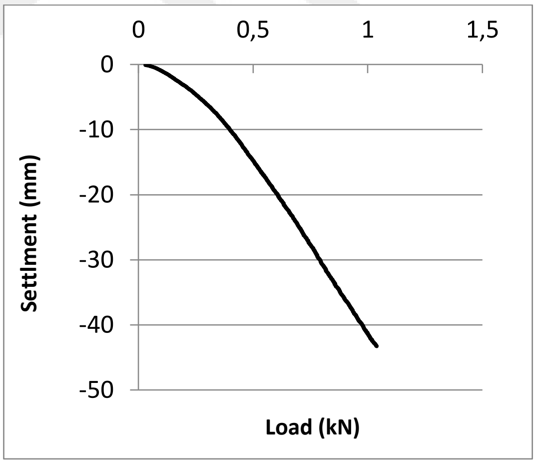

App 1.4 Load-settlement behavior (L=1B, He=1.5B)

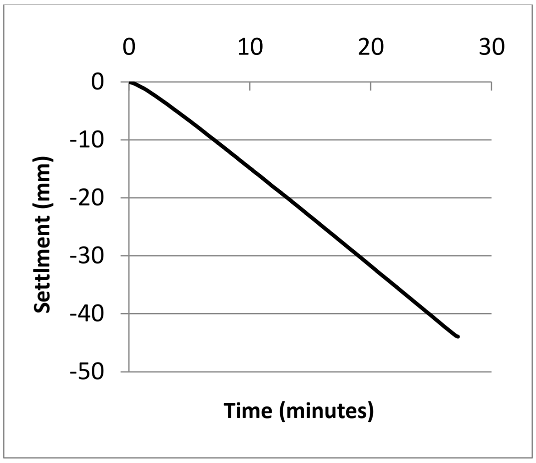

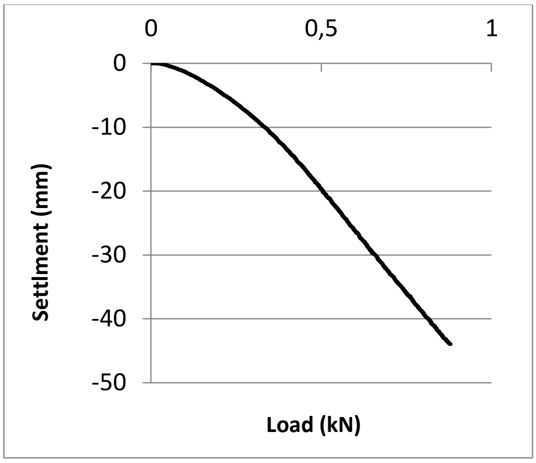

App 1.5 Time-settlement behavior (L=1B, He=2B) **App 1.6** Load-settlement behavior (L=1B, He=2B)

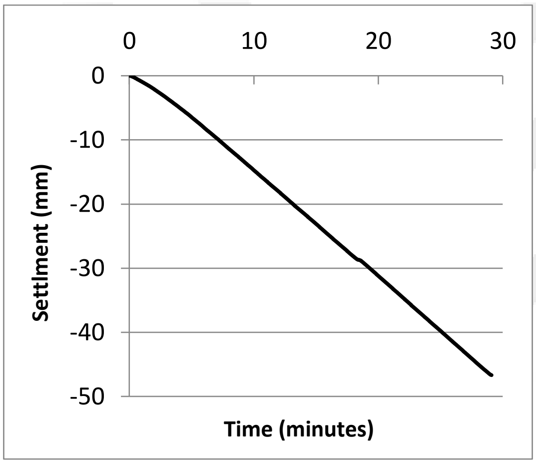

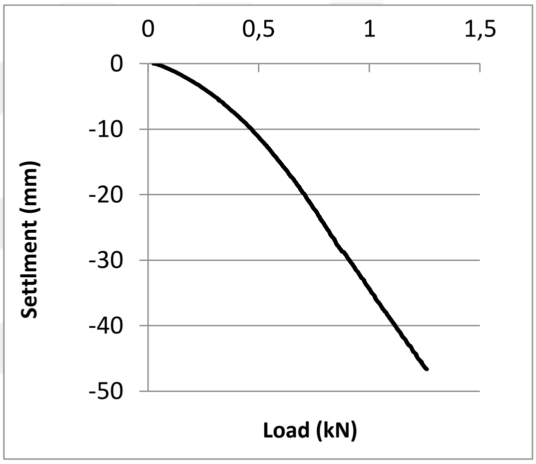

App 1.7 Time-settlement behavior (L=1.5B, He=1B) **App 1.8** Load-settlement behavior (L=1.5B, He=1B)

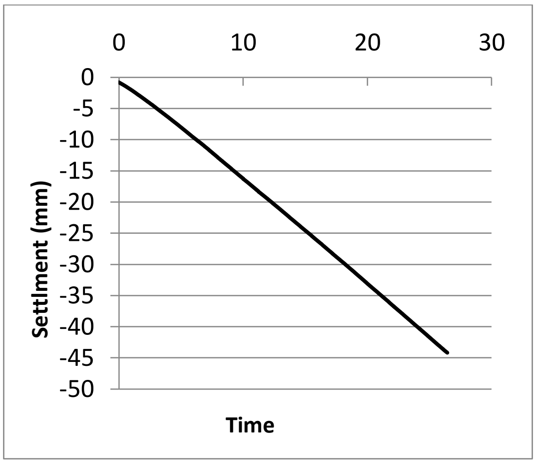

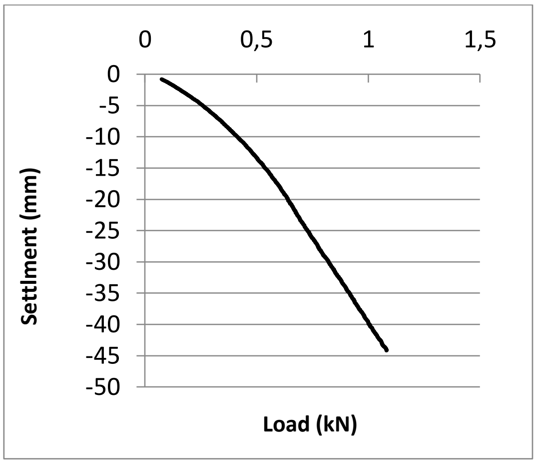

App 1.9 Time-settlement behavior (L=1.5B, He=1.5B) **App 1.10** Load-settlement behavior (L=1B, He=1.5B)

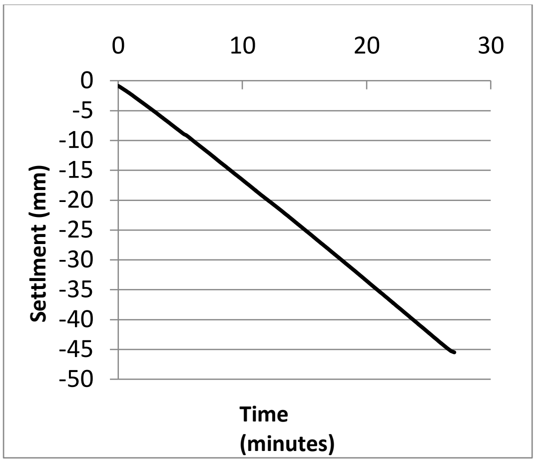

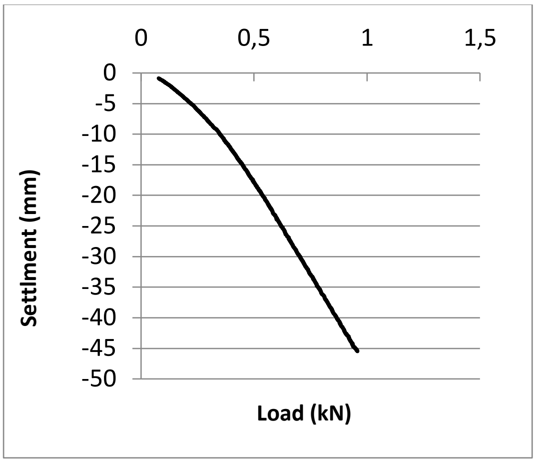

App 1.11 Time-settlement behavior (L=1.5B, He=2B) **App 1.12** Load-settlement behavior (L=1B, He=2B)

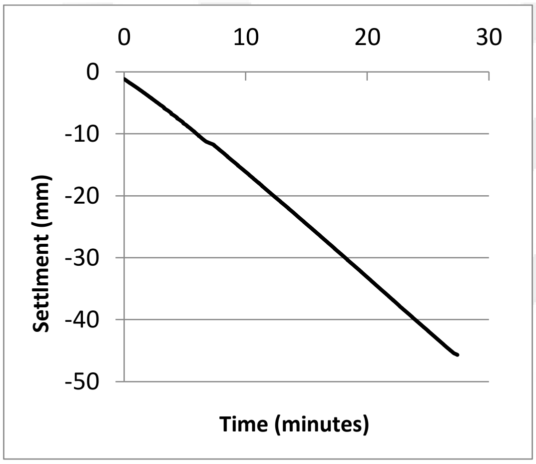

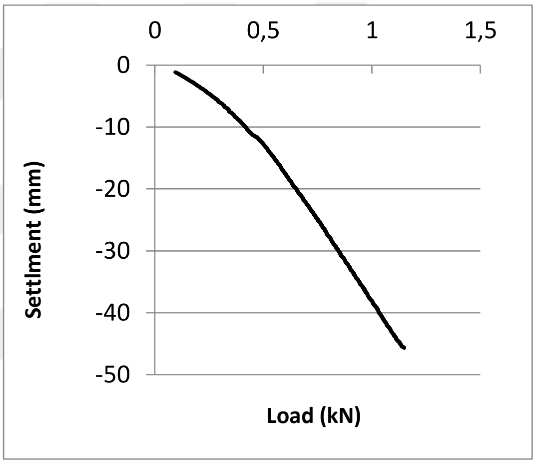

App 1.13 Time-settlement behavior (L=2B, He=1B) **App 1.14** Load-settlement behavior (L=2B, He=1B)

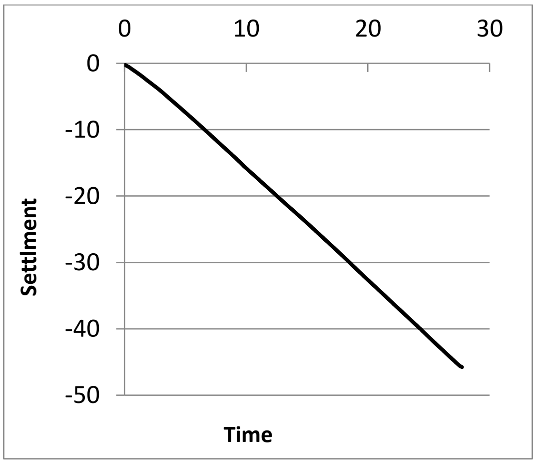

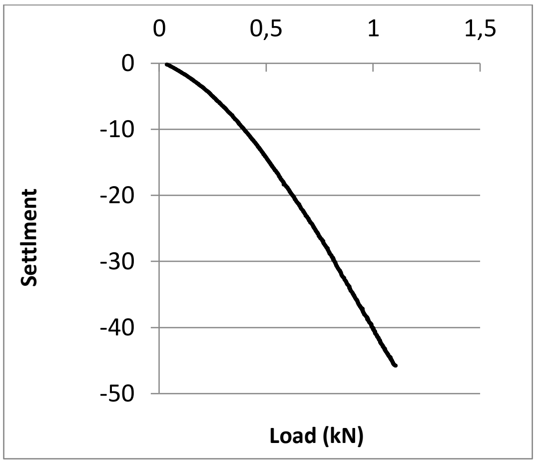

App 1.15 Time-settlement behavior (L=2B, He=1.5B) **App 1.16** Load-settlement behavior (L=2B, He=1.5B)

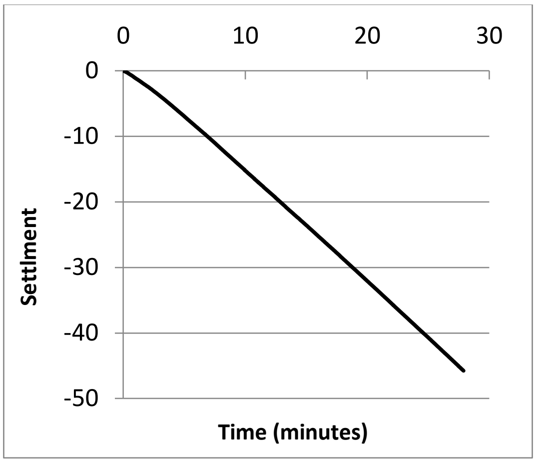

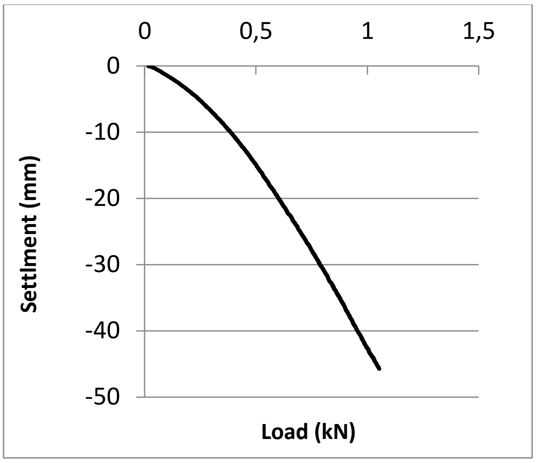

App 1.17 Time-settlement behavior (L=2B, He=2B) **App 1.18** Load-settlement behavior (L=2B, He=2B)

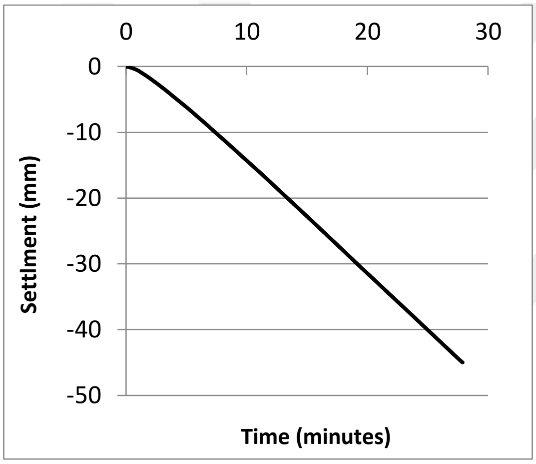

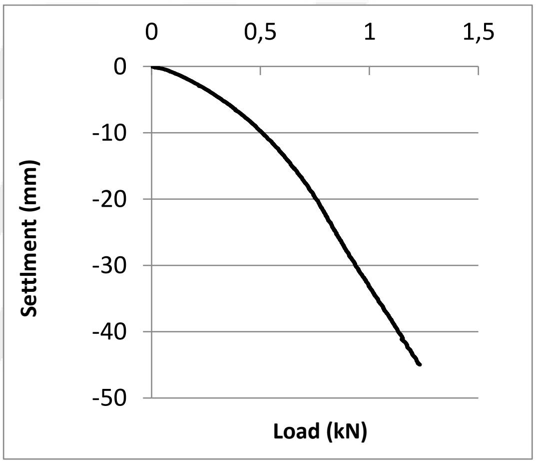

App 1.19 Time-settlement behavior (only foundation model)

App 1.20 Load-settlement behavior (only foundation model)

.

APP-2: EXPERIMENTAL TIME-LOAD OF STEEL FOUNDATION MODEL.

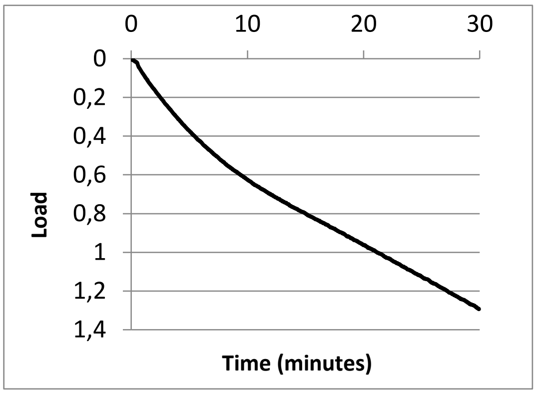

App 2.1 Time-load behavior (L=1B, He=1B)

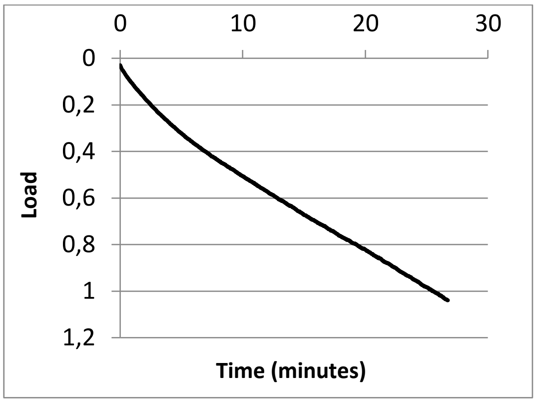

App 2.2 Time-load behavior (L=1B, He=1.5B)

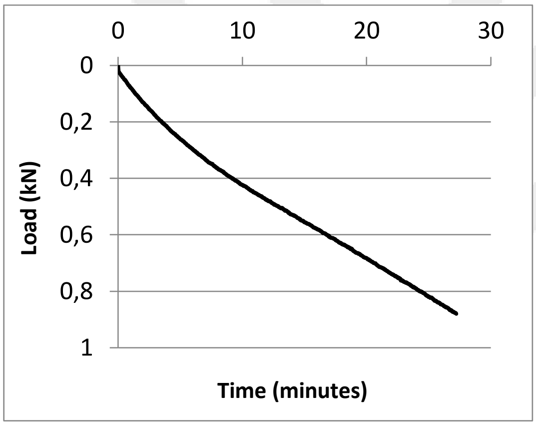

App 2.3 Time-load behavior (L=1B, He=2B)

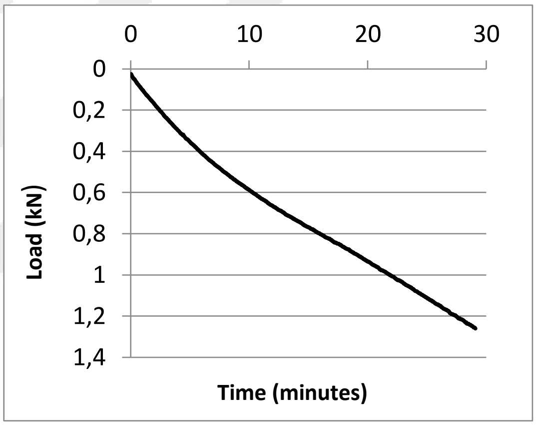

App 2.4 Time-load behavior (L=1.5B, He=1B)

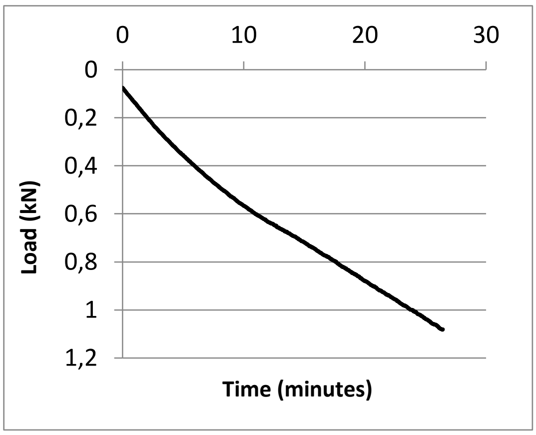

App 2.5 Time-load behavior (L=1.5B, He=1.5B)

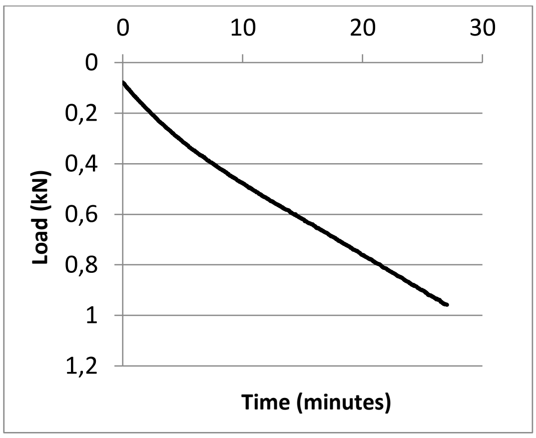

App 2.6 Time-load behavior (L=1.5B, He=2B)

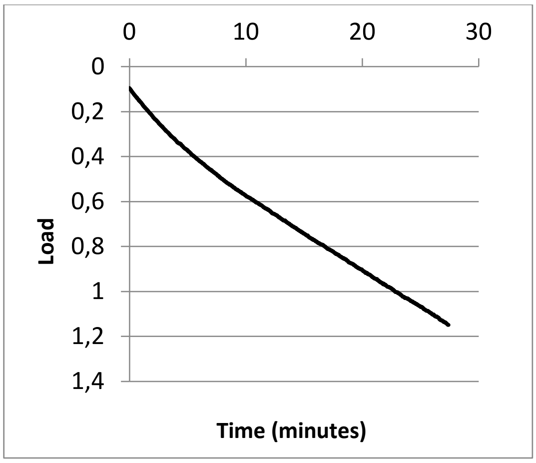

App 2.7 Time-load behavior (L=2B, He=1B)

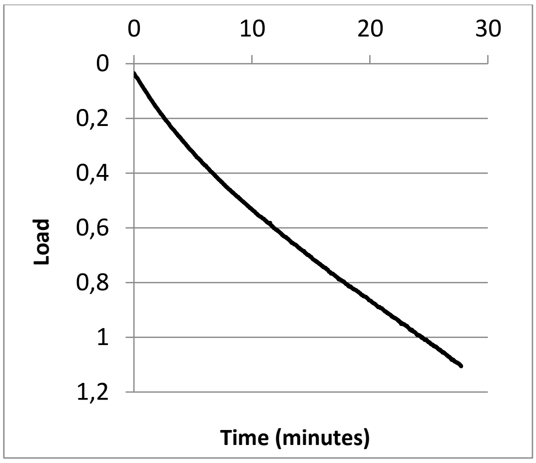

App 2.8 Time-load behavior (L=2B, He=1.5B)

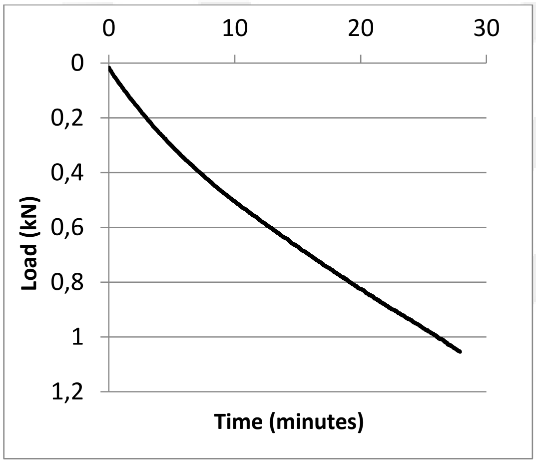

App 2.9 Time-load behavior (L=2B, He=2B)

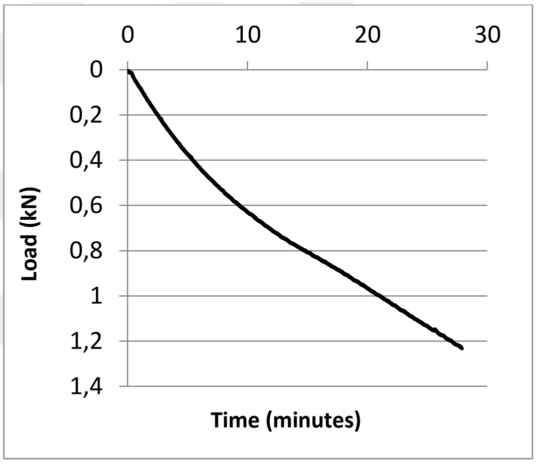

App 2.10 Time-load behavior (only foundation model)

.

APP-3: EXPERIMENTAL TIME-DEFLECTION AND LOAD-DEFLECTION OF SHEET PILE MODEL.

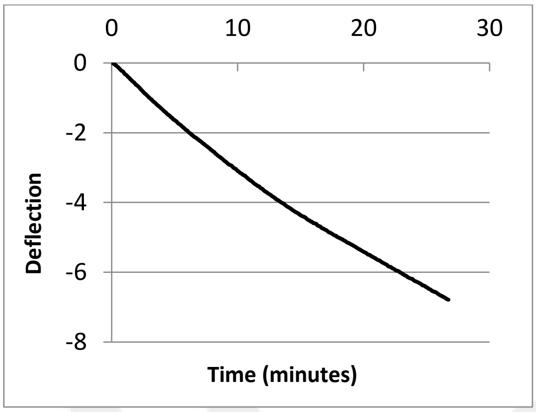

App 3.1 Time-deflection (L=1B, He=1B)

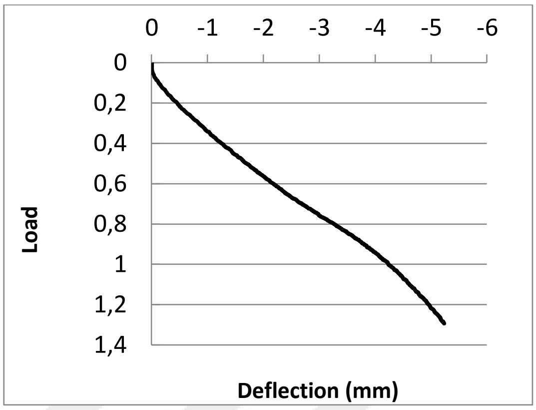

App 3.2 Load-deflection (L=1B, He=1B)

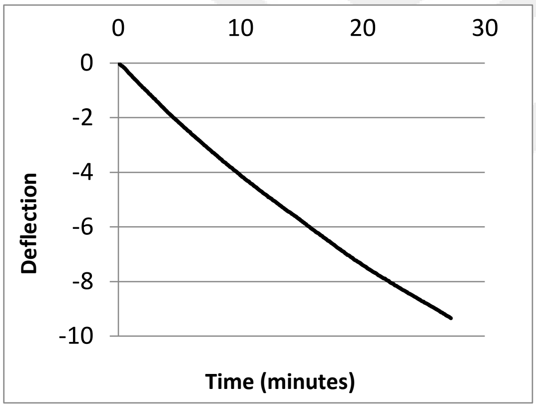

App 3.3 Time-deflection (L=1B, He=1.5B)

App 3.4 Load-deflection (L=1B, He=1.5B)

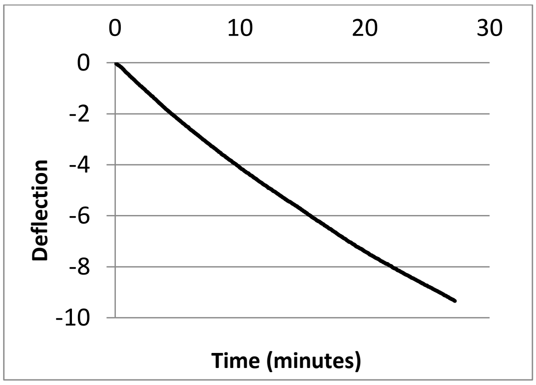

App 3.5 Time-deflection (L=1B, He=2B)

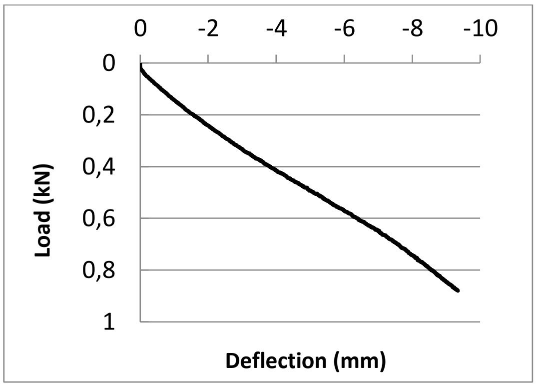

App 3.6 Load-deflection (L=1B, He=2B)

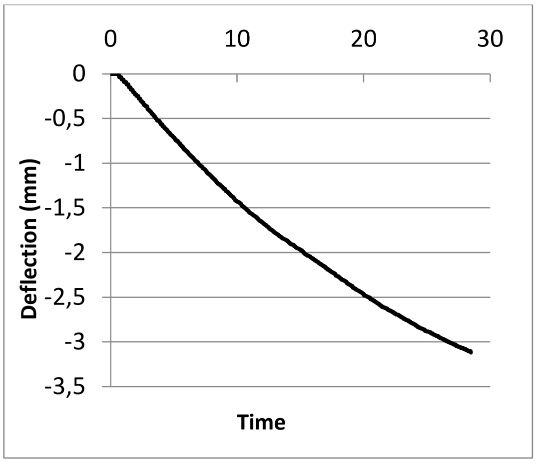

App 3.7 Time-deflection (L=1.5B, He=1B)

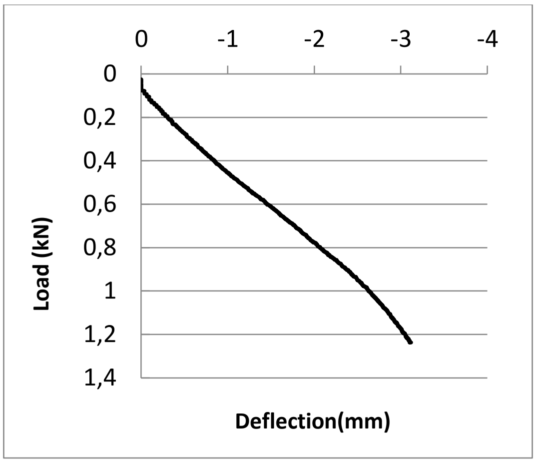

App 3.8 Load-deflection (L=1.5B, He=1B)

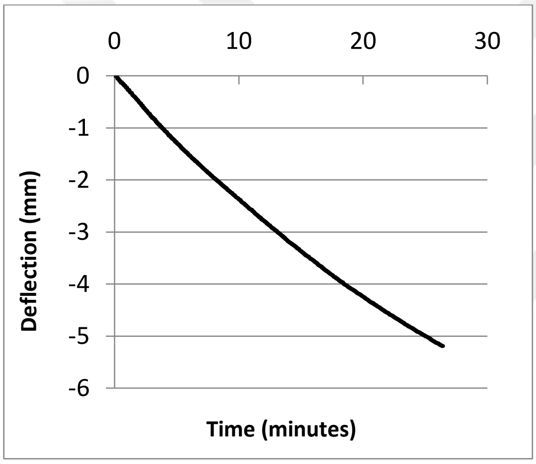

App 3.9 Time-deflection (L=1.5B, He=1.5B)

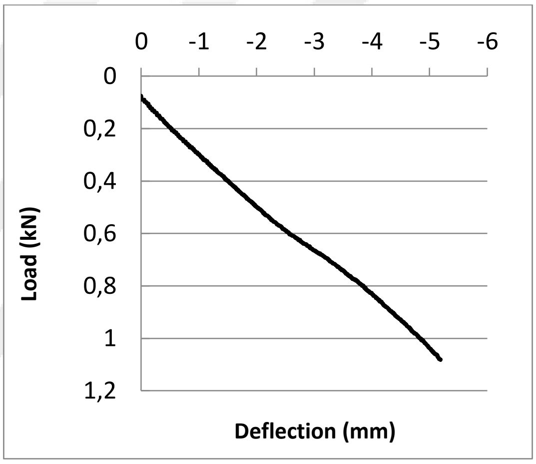

App 3.10 Load-deflection (L=1.5B, He=1.5B)

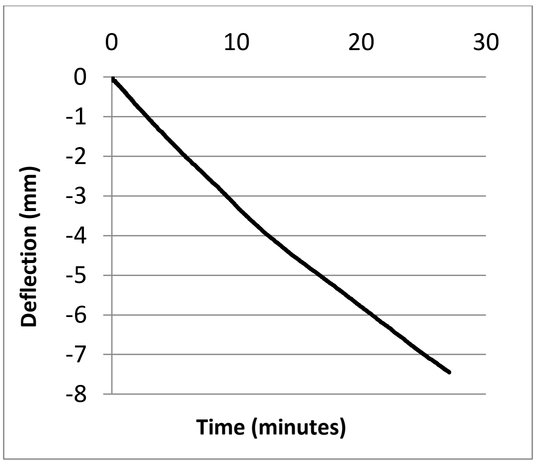

App 3.11 Time-deflection (L=1.5B, He=2B)

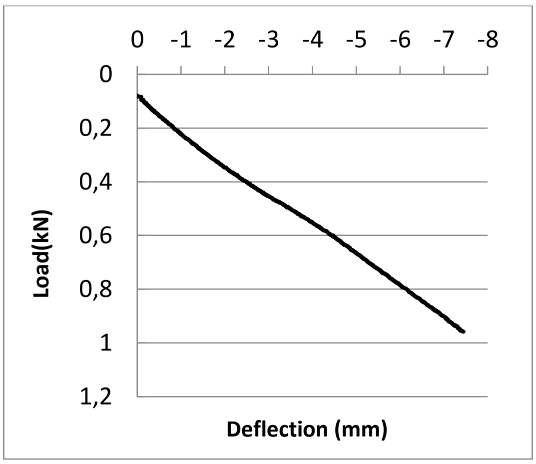

App 3.12 Load-deflection (L=1.5B, He=2B)

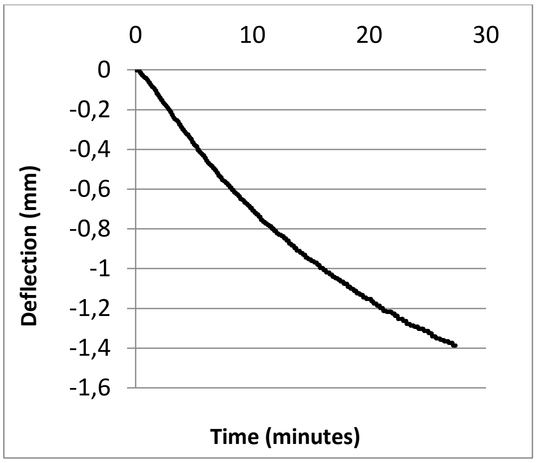

App 3.13 Time-deflection (L=2B, He=1B)

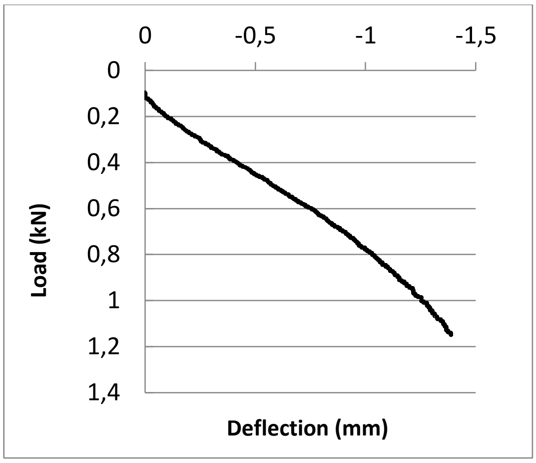

App 3.14 Load-deflection (L=2B, He=1B)

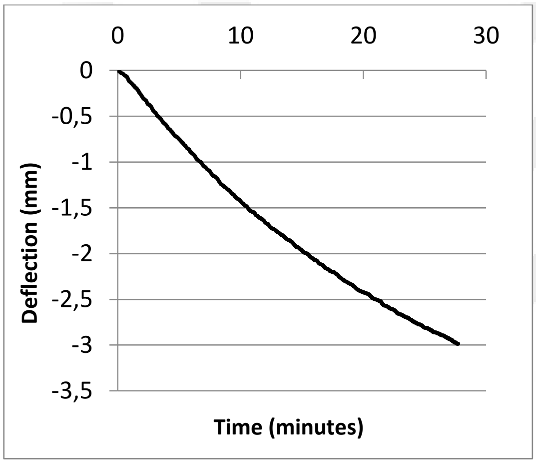

App 3.15 Time-deflection (L=2B, He=1.5B)

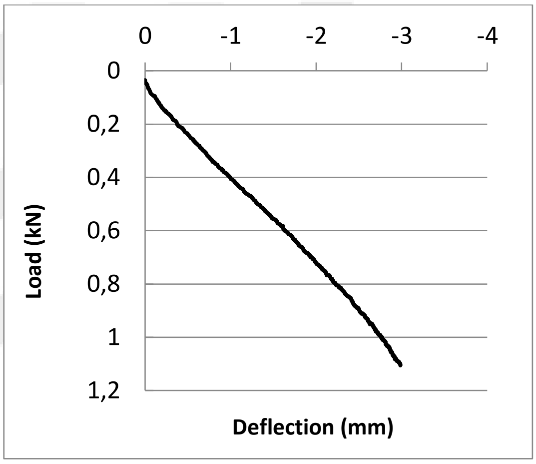

App 3.16 Load-deflection (L=2B, He=1.5B)

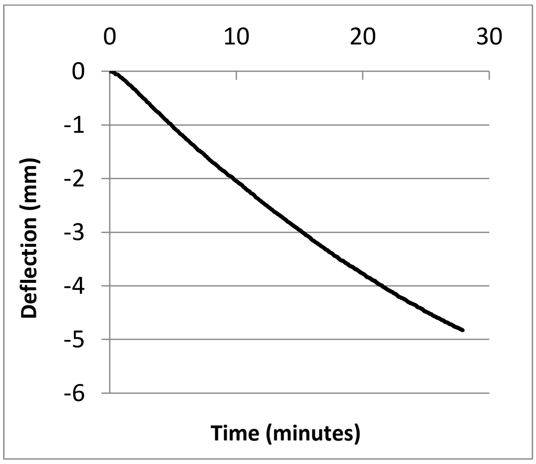

App 3.17 Time-deflection (L=2B, He=B)

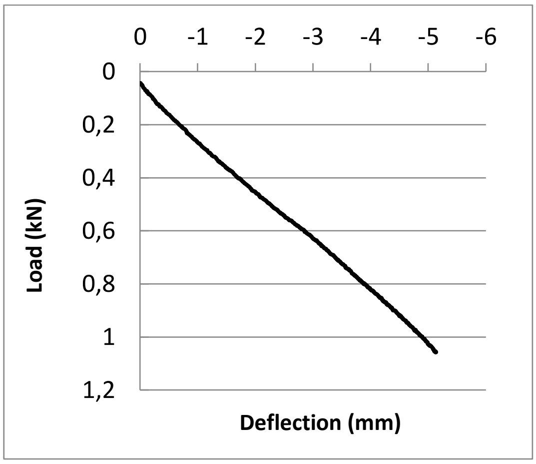

App 3.18 Load-deflection (L=2B, He=2B)

APP-4: EXPERIMENTAL TIME-LATERAL PRESSURE OF SHEET PILE MODEL.

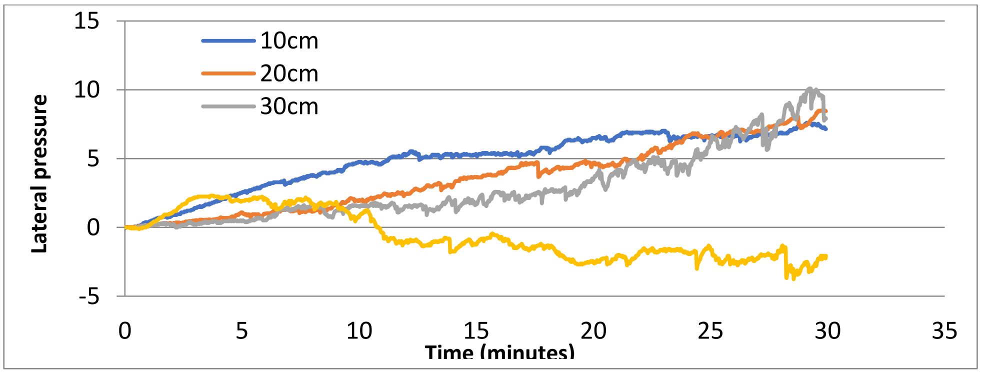

App 4.1 Time-lateral pressure of sheet pile (L=1B, He=1B)

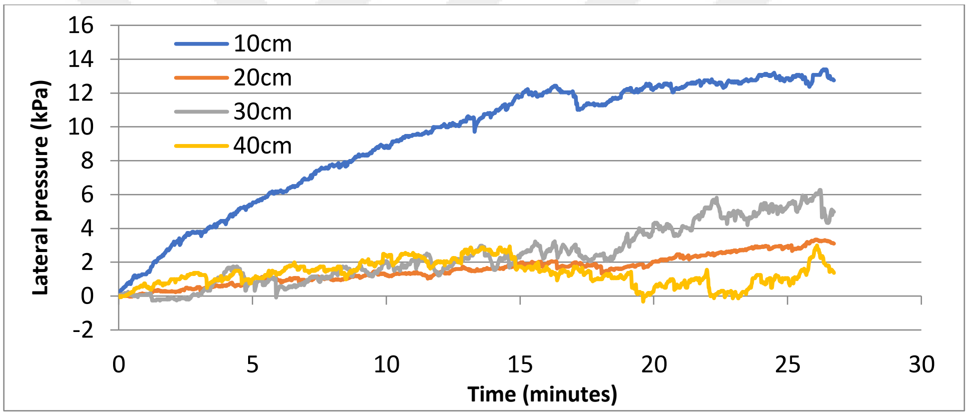

App 4.2 Time-lateral pressure of sheet pile (L=1B, He=1.5B)

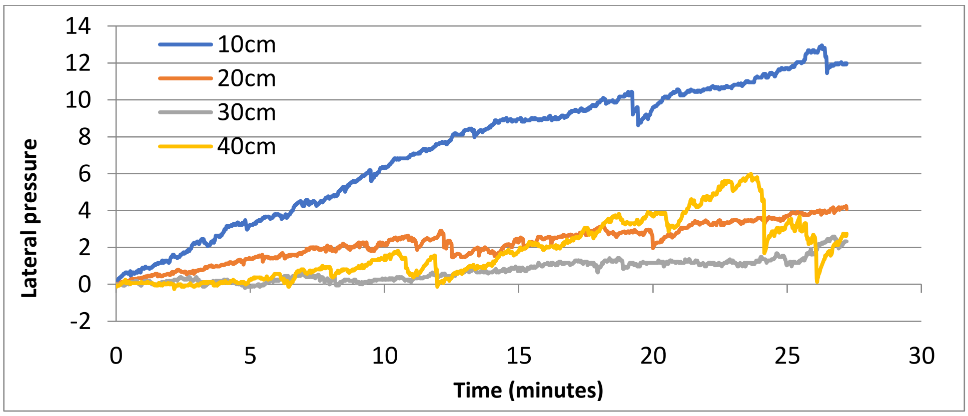

App 4.3 Time-lateral pressure of sheet pile (L=1B, He=2B)

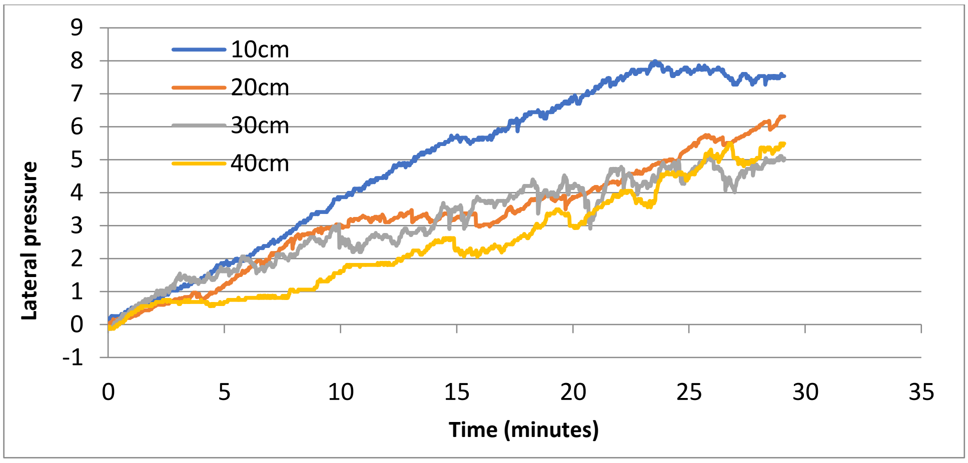

App 4.4 Time-lateral pressure of sheet pile (L=1.5B, He=1B)

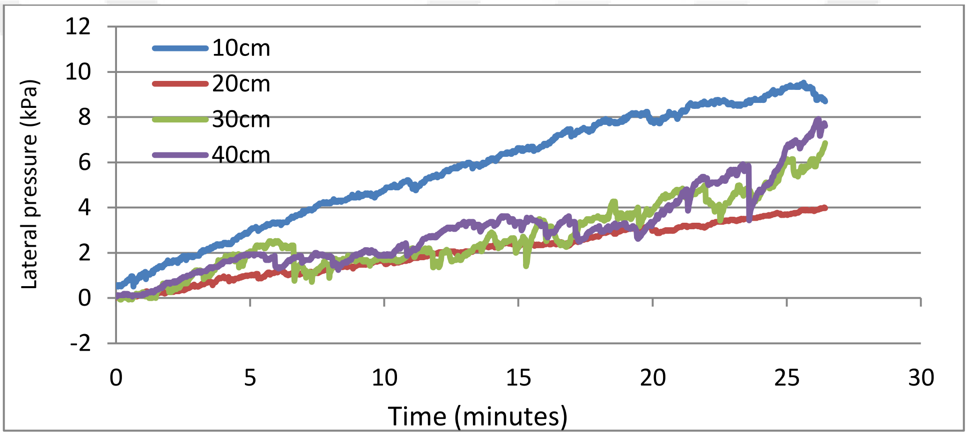

App 4.5 Time-lateral pressure of sheet pile (L=1.5B, He=1.5B)

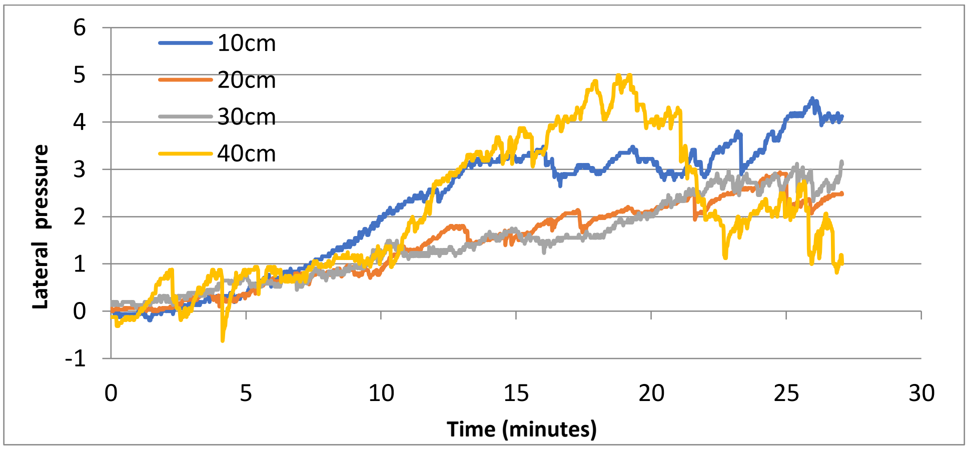

App 4.6 Time-lateral pressure of sheet pile (L=1.5B, He=2B)

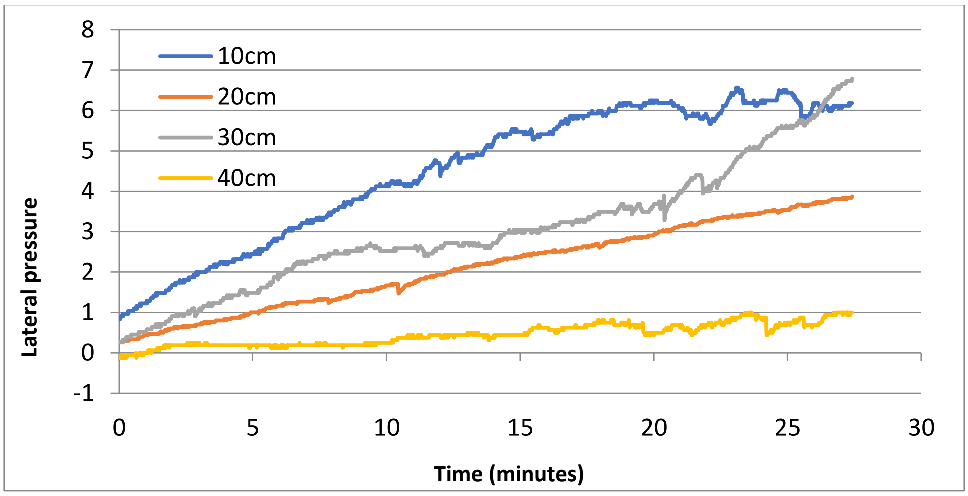

App 4.7 Time-lateral pressure of sheet pile (L=2B, He=1B)

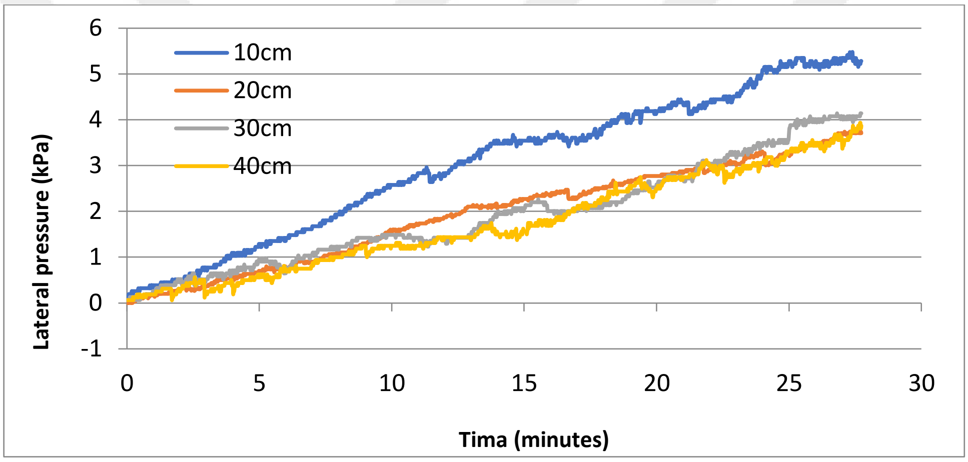

App 4.8 Time-lateral pressure of sheet pile (L=2B, He=1.5B)

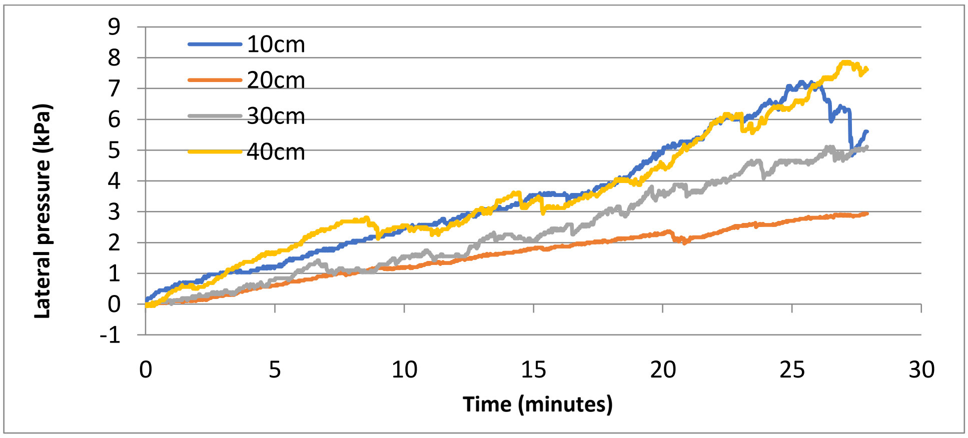

App 4.9 Time-lateral pressure of sheet pile (L=2B, He=2B)

CURRICULUM VITAE

Bedar Rasul MAHMOOD

PERSONAL INFORMATION

Place of Birth : Sulaymani.

Year of Birth : 13/July/1994

Nationality : Iraqi

Address : Sulaymani-Green city

E-mail : bedarrasul@gmail.com

Foreign Languages: English (B2)

Education Information

Bachelor : Sulaymani University, Faculty of Engineering, Department of Irrigation, 2017

High School : Darbandikhan High School-Sulaymani-, 2013